Doctoral Dissertation

Development of Sulfide-based Inorganic-organic Hybrid Solid Electrolytes for All-solid-state Lithium Batteries

University	Hokkaido University
Affiliation	Graduate School of Chemical Sciences and Engineering
Name	Tong FANG
Supervisor	Prof. TADANAGA Kiyoharu

Table of Contents

Chapter 1 Introduction

1.1 Research Background

With the increasing global demand for safer and more efficient energy storage solutions, all-solid-state lithium batteries have emerged as a research hotspot due to their potential for high safety and energy density. This battery technology is particularly suitable for electric vehicles and portable electronic devices, with commercialization anticipation in the coming years. Compared to traditional lithium-ion batteries, all-solid-state lithium batteries offer higher energy density and enhanced safety, especially in terms of mitigating safety risks associated with liquid electrolytes. Consequently, all-solid-state lithium batteries have become a critical direction for future energy storage technology.[1-6]

All-solid-state lithium batteries effectively address the safety issues of flammability and leakage associated with liquid electrolytes by replacing traditional liquid electrolytes with solid-state electrolytes. Solid-state electrolytes also have a wider electrochemical stability window, allowing them to pair with high-energy-density cathode and anode materials, thus further enhancing the battery's energy density. However, despite the unparalleled safety and performance advantages of all-solid-state lithium batteries in theory, their commercial application still faces numerous technical challenges. These challenges mainly include the ionic conductivity of the electrolyte, interfacial stability between the electrolyte and electrode materials, and the optimization of manufacturing costs.[7-10]

Firstly, the performance of all-solid-state lithium batteries is highly dependent on the ionic conductivity of the solid electrolyte. Compared to liquid electrolytes, solid electrolytes typically exhibit lower ionic conductivity. Enhancing ionic conductivity while ensuring material stability is

one of the key factors for the commercialization of all-solid-state lithium batteries. In addition, the interface contact between the solid electrolyte and electrode materials is another major bottleneck affecting the performance of all-solid-state batteries. In these batteries, the interfacial resistance between the electrolyte and electrode is usually high, which can lead to increased internal polarization and, consequently, affect the rate capability and cycle life of the battery. Particularly during charge and discharge cycles, the volume changes of electrode materials can easily cause poor interface contact or even interfacial fractures, severely impacting the stability and lifespan of the battery.[11]

Secondly, the manufacturing process of all-solid-state lithium batteries is more intricate and challenging compared to traditional lithium-ion batteries due to the high requirements for materials and environmental conditions. In particular, during the preparation of solid electrolyte materials and cell assembly, strict environmental control is required to prevent moisture or oxidation of materials. The preparation methods for solid electrolyte materials, such as ball milling, liquid-phase methods, and solid-state reactions, significantly influence their microstructure and ionic conductivity. Historically, melting starting materials to form glass was also extensively studied. Additionally, achieving a compact and stable interface between the solid electrolyte and electrode materials remains a technical challenge. Developing efficient manufacturing processes and equipment is crucial for reducing the production costs of all-solid-state lithium batteries and enabling large-scale production.[10]

Currently, research on all-solid-state lithium batteries primarily focuses on the following areas: developing novel solid electrolyte materials with high ionic conductivity and a wide electrochemical stability window; optimizing the interface between the electrolyte and high-energy-density electrode materials to reduce interfacial impedance and enhance interface stability;

and improving battery assembly processes to increase overall performance and manufacturing efficiency. Continuous innovation and breakthroughs in these areas are expected to significantly enhance the overall performance of all-solid-state lithium batteries, promoting their application in electric vehicles, portable electronic devices, and stationary energy storage systems.

In summary, the development of all-solid-state lithium battery technology is not only crucial for addressing current energy storage challenges but also represents a vital step in advancing the future energy revolution. Research into the key materials, interface optimization, and manufacturing technologies for all-solid-state lithium batteries provides a robust scientific foundation for achieving safer and more efficient energy storage systems. This study, based on these backgrounds, explored the key materials for high-performance all-solid-state lithium batteries and assess their feasibility for practical applications, thereby offering innovative solutions for future energy storage.

1.2 Introduction to All-Solid-State Lithium Batteries

1.2.1 Advantages of All-Solid-State Lithium Batteries

All-solid-state lithium batteries are an electrochemical energy storage system that utilizes solid electrolytes in place of traditional liquid electrolytes, offering significant advantages over conventional lithium-ion batteries in terms of safety, energy density, and cycle life. A key characteristic of all-solid-state lithium batteries is the use of solid electrolytes, which provide excellent mechanical stability and high electrochemical stability.[12] Conventional lithium-ion batteries use flammable organic liquid electrolytes, which can leak and ignite if the battery is physically damaged or experiences an internal short circuit, creating potential safety hazards. In contrast, all-solid-state batteries utilize non-flammable solid electrolytes, effectively mitigating these risks and significantly enhancing battery safety. Additionally, all-solid-state lithium batteries offer an advantage in energy density, particularly when lithium metal is used as the anode material. Lithium metal has a theoretically specific capacity of up to 3860 mAh/g, approximately ten times that of traditional graphite anodes, giving all-solid-state lithium batteries exceptionally high energy density. Furthermore, the wide electrochemical stability window of solid electrolyte materials allows them to pair well with high-voltage cathode materials, further increasing the battery's energy output.

Currently, research on all-solid-state lithium batteries focuses primarily on the development and improvement of solid electrolyte materials, which are mainly categorized into inorganic and polymer electrolytes. Inorganic electrolytes include oxides, sulfides, and halides. Sulfide electrolytes have gained considerable attention due to their high ionic conductivity and favorable mechanical properties, while oxide electrolytes are known for their excellent chemical stability, although their ionic conductivity is relatively low. Polymer electrolytes, on the other hand, offer

good flexibility and processability, but their ionic conductivity is generally low at room temperature, limiting their application in high-performance batteries.

In addition to the development of solid electrolyte materials, interface optimization is another critical area of research in all-solid-state lithium batteries. The high interfacial resistance between the electrolyte and the electrode is primarily caused by poor physical contact, mismatched mechanical properties, interfacial chemical reactions, and limited ionic transport. These issues result in increased internal polarization, thereby affecting the battery's rate performance and cycling stability. Particularly during charge and discharge cycles, electrode materials undergo volume changes, which may result in poor contact or even fractures at the electrolyte-electrode interface. Therefore, improving interfacial compatibility and stability between electrolyte and electrode materials is crucial for achieving high-performance all-solid-state lithium batteries. Many current studies focus on reducing interfacial impedance and enhancing interface stability through methods such as interface modification and the introduction of intermediate layers to improve the overall performance of all-solid-state lithium batteries.[13]

In addition, the manufacturing process of all-solid-state lithium batteries is another critical factor impacting their commercialization. Compared to traditional lithium-ion batteries, the manufacturing of all-solid-state batteries requires more stringent processes and environmental conditions. For instance, solid electrolyte materials must be prepared and processed in strictly anhydrous and oxygen-free environments, particularly for sulfide electrolytes, as exposure to air can degrade their performance or even release harmful gases. The manufacturing process involves complex steps such as high-temperature sintering and vacuum drying, requiring precise control of parameters like temperature and pressure to ensure material purity and performance. With advancements in materials science and manufacturing technology, these challenges are gradually

being addressed, leading to reduced production costs, improved efficiency, and accelerated commercialization of all-solid-state lithium batteries.

In summary, all-solid-state lithium batteries, with their superior safety, high energy density, and long cycle life, are strong candidates for next-generation energy storage systems. Although technical challenges remain in material development, interface optimization, and manufacturing processes, ongoing research and technological breakthroughs are steadily improving the performance of all-solid-state lithium batteries, bringing them closer to the goal of large-scale commercial applications. This study explored the preparation of novel solid electrolyte materials and their applications in all-solid-state lithium batteries, based on the current state of all-solid-state lithium battery technology, aiming to provide innovative solutions for the development of high-performance batteries in the future.

1.2.2 Current Research Status of All-Solid-State Lithium Batteries

Driven by the advantages of solid-state lithium batteries, global research institutions and well-known companies are accelerating their research and commercialization efforts. [14] Toyota is working with companies like Idemitsu to develop high-performance solid electrolytes and other key materials, aiming to overcome current technical bottlenecks, increase energy density, and reduce production costs, with plans to achieve commercialization of solid-state batteries between 2027 and 2028.[15] In November 2024, QuantumScape and PowerCo, a subsidiary of Volkswagen Group, reached a key agreement aimed at accelerating the commercialization of QuantumScape's solid-state lithium metal battery technology. Under this agreement, the two parties will collaborate to manufacture battery cells based on QuantumScape's technology and establish a large-scale team to jointly develop production processes. This agreement is a significant part of QuantumScape's commercialization strategy, showcasing QuantumScape's cutting-edge technology and PowerCo's

global industrialization capabilities, while significantly reducing the time and difficulty of scaling production to market through a capital-light business model. [16] Through these continuous efforts, the global battery industry is gradually pushing solid-state battery technology from laboratory research to large-scale production, meeting the growing demand for high-performance battery technology in the global electric vehicle market.

Among solid electrolytes, Sulfide electrolytes exhibit excellent ionic conductivity and interfacial properties, but their environmental stability issues still need to be addressed through coating techniques and anhydrous processes. Oxide electrolytes are well-known for their chemical stability, but their relatively low ionic conductivity presents a significant limitation. Techniques such as doping and grain boundary optimization are being widely applied to enhance their conductivity while retaining their inherent stability. Polymer electrolytes, with their flexibility and processability, hold advantages in certain applications, but their insufficient ionic conductivity at room temperature limits their broader use. Developing inorganic-polymer composite electrolytes or hybrid electrolytes has emerged as a key direction for improving performance. At the same time, interfacial resistance remains a critical challenge for all types of solid electrolytes. To address this issue, researchers are focusing on strategies such as introducing functionalized interlayers, optimizing the mechanical properties of electrolytes, and applying novel interfacial modification techniques. These approaches have proven effective in enhancing interfacial stability, reducing resistance, and improving the cycling performance and rate capabilities of batteries.

In terms of battery improvement, researchers are continuously exploring new strategies to enhance the energy density and cycle life of all-solid-state lithium batteries. For instance, optimizing the stacking of electrode materials and current distribution within the battery can effectively reduce internal polarization. Additionally, advancements in modular approaches are

rapidly providing more efficient solutions for electric vehicles and other high-energy-demand applications.

The market potential and application fields of all-solid-state lithium batteries are extensive. From electric vehicles to portable electronic devices and large-scale energy storage systems, all-solid-state lithium batteries are expected to provide more efficient and safer energy storage solutions for these fields. As technology matures and production costs decrease, all-solid-state batteries are likely to achieve widespread commercialization within the next decade. Particularly in the electric vehicle sector, all-solid-state batteries are expected to significantly enhance driving range and safety. Furthermore, portable electronics, as well as residential and industrial energy storage systems, benefit from the high energy density and long cycle life offered by all-solid-state batteries.

In conclusion, although research and development of all-solid-state lithium batteries still face numerous technical challenges, their remarkable advantages in safety, energy density, and environmental adaptability make them a crucial direction for future energy storage technology. With the combined efforts of global research institutions, commercial companies, and startups, the performance of all-solid-state batteries is steadily improving, and the goal of large-scale commercialization is coming closer. As research progresses and breakthroughs are achieved, all-solid-state lithium batteries are poised to become a key driving force in the modern energy revolution, offering robust solutions to global energy challenges.

1.3 Introduction to Solid Electrolyte Materials

As discussed in the previous section, solid electrolyte materials are a core component of all-solid-state lithium batteries. They primarily serve as the conductive medium for lithium ions while isolating the cathode and anode to prevent short internal circuits. To build on the earlier discussion, this section further elaborates on the diverse types of solid electrolyte materials, including inorganic solid electrolytes (such as oxides and sulfides), polymer electrolytes, and inorganic-organic composite/hybrid electrolytes. Each material offers unique characteristics and advantages, contributing indispensably to the advancement of all-solid-state lithium batteries. [1, 17]

Inorganic solid electrolytes are mainly classified into oxide electrolytes, sulfide electrolytes, and halide electrolytes. Among them, oxide solid electrolytes exhibit excellent chemical stability and a wide electrochemical stability window, effectively preventing irreversible reactions with lithium metal anodes, thus demonstrating exceptionally high safety. Common oxide electrolytes include perovskite-structured $Li_{3x}La_{2/3-x}TiO_3$ (LLTO) and cubic-structured $Li_7La_3Zr_2O_{12}$ (LLZO). While these materials perform well in terms of chemical stability, their ionic conductivity is relatively low, particularly at room temperature, making it difficult to reach the conductivity levels of liquid electrolytes. Therefore, improving the room-temperature conductivity of oxide electrolytes is one of the current research focuses.[18]

Sulfide solid electrolytes, due to their high ionic conductivity and good mechanical flexibility, have become a key focus in all-solid-state lithium battery research. Typical sulfide electrolytes include $Li_{10}GeP_2S_{12}$ (LGPS) and Li_6PS_5X (X = Cl, Br, I). The ionic conductivity of these sulfide electrolytes at room temperature can reach between 10^{-3} S cm^{-1} and 10^{-2} S cm^{-1}, which is comparable to or even exceeds the level of traditional liquid electrolytes. Additionally, sulfide electrolytes exhibit low interfacial resistance and are compatible with both lithium metal anodes

and high-voltage cathodes. However, sulfide electrolytes are extremely sensitive to moisture, prone to hydrolysis that generates toxic hydrogen sulfide (H_2S), which restricts their operational conditions in practical production and application. Therefore, enhancing the environmental stability of sulfide electrolytes is crucial for their large-scale application.[19]

Polymer solid electrolytes have garnered attention due to their good processability and mechanical flexibility. Common polymer electrolytes, such as polyethylene oxide (PEO)-based electrolytes, typically enhance their ionic conductivity by doping lithium salts into the polymer matrix. These electrolytes are flexible and can be easily prepared in thin-film form, enabling good electrode-electrolyte interface contact and reducing interfacial resistance. However, the ionic conductivity of polymer electrolytes at room temperature is relatively low, generally below 10^{-5} S cm^{-1}, which limits their application in high-energy-density batteries. To address this, researchers are exploring methods such as incorporating nanofillers, creating composites, and crosslinking to improve the room-temperature conductivity and mechanical strength of polymer electrolytes.[20]

Inorganic-organic composite electrolytes aim to combine the high ionic conductivity of inorganic electrolytes with the high flexibility of polymer electrolytes. These composite materials are typically prepared through physical methods, such as dispersing inorganic nanoparticles within a polymer matrix or coating polymer layers onto the surfaces of inorganic materials. This approach significantly enhances the overall performance of the electrolyte, achieving a balance between ionic conductivity, interfacial compatibility, and mechanical properties. Additionally, another important class of materials related to composite electrolytes is inorganic-organic hybrid electrolytes, which are integrated at the molecular or nanoscale through chemical methods, often involving the formation of chemical bonds. This chemical integration further improves interfacial stability and overall performance. Although composite and hybrid electrolytes share some

similarities in their objectives and structures, they differ significantly in their preparation methods and material characteristics. In recent years, both types of materials have emerged as critical research focuses in all-solid-state lithium batteries due to their potential for high performance and broad application prospects.[21]

In addition to material types, the ionic conduction mechanism of solid electrolytes is also a key research focus. In solid electrolytes, lithium ions typically conduct through vacancies or interstitial sites within the lattice. For crystalline electrolytes, ion conduction mainly relies on defects and channels within the lattice structure, while in amorphous or glassy electrolytes, ions diffuse through the disordered structure of the amorphous network. Therefore, optimizing the structure of solid electrolytes to enhance defect density and connectivity of conduction pathways is an effective approach to improving ionic conductivity.

In the study of solid electrolytes, there is often a trade-off between ionic conductivity and chemical stability. Highly conductive materials are often chemically less stable—for instance, sulfide electrolytes are sensitive to moisture and air—while materials with high chemical stability, such as certain oxide electrolytes, often exhibit suboptimal ionic conductivity. Balancing these two properties is a core challenge in solid electrolyte research. Additionally, the mechanical properties of solid electrolytes are crucial, as the electrolyte in all-solid-state batteries must not only have good ionic conductivity but also withstand electrode volume changes during charge and discharge cycles without cracking.

Significant progress has already been made in the research of solid electrolyte materials. For example, methods such as doping, compositing, and lattice design have allowed researchers to improve the ionic conductivity and chemical stability of various solid electrolytes. Moreover, the emergence of novel electrolyte materials, such as perovskite-structured oxides, superionic sulfides,

and new composite electrolytes, has opened up new possibilities for the development of all-solid-state lithium batteries. In the future, with deeper understanding of solid electrolyte materials and the continuous emergence of new materials and techniques, breakthroughs in energy density, safety, and cycle life of all-solid-state lithium batteries are expected.

In summary, solid electrolyte materials are at the core of all-solid-state lithium battery technology, directly determining the overall performance and commercialization prospects of the battery. Through the development and improvement of various types of solid electrolytes—including oxides, sulfides, polymers, and inorganic-organic composites—researchers continue to explore ways to enhance ionic conductivity, chemical stability, and mechanical properties, thereby laying a solid foundation for the practical application of all-solid-state lithium batteries. This study focused on novel sulfide-based solid electrolytes, exploring their applications in all-solid-state lithium batteries and their potential for enhancing overall battery performance.

1.4 Development History and Challenges of Sulfide Solid Electrolytes

Sulfide solid electrolytes have played a significant role in the development of all-solid-state lithium batteries, with research dating back to the 1980s. Initially, researchers attempted to mix Li_2S and P_2S_5, resulting in a sulfide solid electrolyte with an amorphous, glassy structure and an ionic conductivity of approximately 10^{-4} S cm^{-1}.[22] These early studies laid the foundation for solid electrolytes. However, due to the dominance of liquid electrolytes in the market, attributed to their higher conductivity and lower cost, research on sulfide electrolytes experienced a period of stagnation.

It was not until the early 2000s, with the growing demand for high-safety, high-energy-density batteries, that research on sulfide solid electrolytes regained attention. In 2001, the thio-LISICON (thio-Lithium Superionic Conductor) structure Li_2S-P_2S_5 binary sulfide solid electrolyte material was introduced, marking the beginning of a significant surge in the development of high-conductivity sulfide solid electrolytes.[23] In 2005, a $70Li_2S$-$30P_2S_5$ glass-ceramic electrolyte was reported, [24] and in 2007, a high-temperature conducting phase of the Li_2S-P_2S_5 system, $Li_7P_3S_{11}$, was introduced. [25] Both exhibited conductivities reaching 10^{-3} S cm^{-1}. Subsequently, the argyrodite-type electrolyte system (Li_6PS_5X, X = F, Cl, Br, I) demonstrated high ionic conductivities in the range of 1-10 mS cm^{-1}, as reported by Hans-Jorg Deiseroth and colleagues in 2008. [26] In 2011, $Li_{10}GeP_2S_{12}$ (LGPS) was developed, achieving an ionic conductivity of 12 mS cm^{-1} at room temperature, far surpassing most liquid electrolytes available at the time. [27] This breakthrough brought sulfide solid electrolytes back into the spotlight, establishing them as a key focus in all-solid-state lithium battery research.

In recent years, significant progress has also been made in the further development of sulfide-based solid electrolytes. For example, the material $Li_{9.54}Si_{1.74}P_{1.44}S_{11.7}Cl_{0.3}$ has demonstrated an

ionic conductivity as high as 20 mS cm^{-1}, one of the highest conductivities reported to date among sulfide-based electrolytes.[28] In addition, single crystals of $Li_{10}GeP_2S_{12}$ have achieved conductivity as high as 27 mS cm^{-1} along the [001] direction, demonstrating the exceptionally high ion migration capability of sulfide materials in specific orientations.[29]

However, sulfide electrolytes also face numerous challenges. Firstly, they are highly sensitive to moisture, easily reacting with water to produce toxic hydrogen sulfide (H_2S), which poses safety risks in terms of material preparation, storage, and processing. Secondly, irreversible chemical reactions may occur when sulfide electrolytes are in contact with electrode materials, leading to interface degradation. This is especially problematic with lithium metal or silicon anodes, as their significant volume changes during charge and discharge cycles can cause stress concentration, leading to cracks in the sulfide electrolyte. In addition, while sulfide electrolytes are relatively soft and can partially alleviate stress caused by electrode volume changes, their mechanical strength remains insufficient. Under prolonged cycling or concentrated stress, they may develop cracks, disrupting interfacial contact and affecting the cycle life of the battery.

To address these issues, researchers have proposed various improvement strategies. For example, protective layers can be introduced between the electrolyte and electrodes, chemical modifications can be applied to the electrolyte, or new composite electrolytes can be developed to enhance interfacial stability. Nanostructuring the material, adding flexible components, or using inorganic-organic composites/hybrids have been explored as effective strategies to improve the mechanical performance of sulfide electrolytes. Additionally, doping with elements such as germanium (Ge), tin (Sn), and indium (In) can not only improve ionic conductivity but also enhance the chemical stability (reducing sensitivity to moisture and air), structural stability (minimizing cracks and structural damage), and interfacial stability (reducing interfacial reactions and impedance

formation). Additionally, replacing some anions in the sulfide electrolyte with fluorine, chlorine, bromine, or iodine can effectively tune the crystal structure and ion migration pathways, thereby enhancing overall material performance.

In addition to advancements in materials and synthesis methods, the application of sulfide electrolytes in battery design has made significant progress. To address the mechanical stress caused by electrode volume changes during cycling, researchers have proposed the introduction of flexible interlayers between the electrolyte and electrode. This approach effectively mitigates mechanical stress and significantly enhances interfacial stability and cycle life of the battery. [30] Meanwhile, to resolve the inherent mechanical brittleness of sulfide electrolytes, researchers have developed composite materials based on polymer matrices and flexible fillers. For instance, by embedding polymer components into sulfide electrolytes, flexible solid electrolyte films can be fabricated to improve material flexibility and adaptability during charge-discharge cycles. This design greatly enhances the stability of the electrolyte-electrode interface and demonstrates outstanding performance in improving the cycling stability of all-solid-state lithium batteries.[31]

The industrialization of sulfide solid electrolytes also faces challenges. Although considerable progress has been made in fundamental research, there remains a significant gap between laboratory-scale studies and large-scale industrial production. Firstly, the synthesis of high-purity sulfide electrolytes is complex and costly, which limits the economic feasibility of large-scale applications. Secondly, the environmental sensitivity of sulfide materials during battery assembly necessitates handling in an anhydrous, oxygen-free environment, which adds further complexity and cost to production.

To address these challenges, research is focusing on developing more cost-effective synthesis methods. For example, liquid-phase synthesis combined with rapid solidification techniques can

reduce costs while maintaining material performance. Researchers are also exploring automation and modular production methods to enhance efficiency and consistency in manufacturing, thus lowering the barriers and costs associated with industrialization. These efforts aim to gradually bridge the gap between fundamental research on sulfide solid electrolytes and commercial-scale production.

In terms of applications, the potential use of sulfide solid electrolytes extends beyond lithium-ion batteries. In emerging energy storage systems such as sodium-ion batteries and magnesium-ion batteries, sulfide electrolytes also show promising application prospects. Especially in sodium-ion batteries, the high ionic conductivity and low interfacial resistance of sulfide electrolytes make them strong candidates to replace conventional liquid electrolytes. Additionally, sulfide electrolytes are well-suited for flexible and micro-battery applications, offering improved safety and longer cycle life for these novel energy storage devices.

In summary, sulfide solid electrolytes show great potential in all-solid-state lithium batteries due to their high ionic conductivity and good interfacial compatibility. However, challenges such as poor air stability, complex interfacial reactions, and weak mechanical properties remain significant barriers to their commercialization. Future research needs to focus on further optimizing the stability and mechanical performance of these materials and developing cost-effective, high-performance synthesis methods to promote the widespread application of sulfide solid electrolytes in all-solid-state batteries. Additionally, more innovative strategies in practical battery design are required to enhance the overall performance and safety of batteries, thereby accelerating the commercialization of all-solid-state lithium batteries.

1.5 Research Motivation and Content of This Study

In the development of all-solid-state batteries, improving energy density and safety has always been a core goal, especially with the growing demand for high-performance applications such as electric vehicles. Developing new, efficient electrolytes has become a major research direction. As a key component, solid electrolytes not only have a decisive impact on the overall battery performance but are also crucial for their long-term stability and safety. In recent years, sulfide-based solid electrolytes have received widespread attention due to their high ionic conductivity; however, when combined with high-capacity silicon anodes, the severe volume changes of silicon during charge and discharge often lead to interfacial cracking, affecting the cycle stability and lifespan of the battery. Therefore, developing solid electrolytes with high flexibility that can effectively accommodate electrode volume changes is key to advancing all-solid-state battery technology.

Based on this, the present study proposes developing a novel organic-inorganic hybrid solid electrolyte by introducing organic cations into sulfide-based electrolytes, aiming to enhance their flexibility and adaptability to accommodate the volume changes of silicon anodes during charge and discharge. The core of this strategy lies in the inclusion of organic cations, which enhances the mechanical flexibility of the electrolyte, enabling it to better adapt to electrode volume changes and effectively reduce interfacial stress. To prepare the solid electrolyte materials, the ball milling method was chosen primarily due to its ability to significantly reduce particle size, thereby increasing the interfacial contact between electrolyte and electrode materials and enhancing ionic conductivity. Compared to the liquid-phase method, which typically results in lower ionic conductivity and involves more complex handling, ball milling provides a more efficient and practical approach for achieving high-performance solid electrolytes. This approach is expected to

improve not only the energy density and cycle stability of all-solid-state batteries but also significantly enhance their overall safety.

Previous studies have shown that introducing tetraethylammonium iodide (TEAI) and tetramethylammonium iodide (TMAI) into AgI-CsI glass systems can significantly enhance ionic conductivity at room temperature, providing important theoretical and practical insights for this research. [32] Based on this, I hypothesize that incorporating tetraalkylammonium ions into sulfide-based electrolytes can create efficient lithium-ion conduction pathways within the glass matrix and improve the mechanical flexibility of the electrolyte. Due to their larger size and low charge density, tetraalkylammonium ions can create a more open structure in the electrolyte, facilitating the migration of free lithium ions.

This study prepared a series of organic-inorganic hybrid sulfide solid electrolytes to explore their potential in enhancing the performance of all-solid-state batteries. Specifically, I systematically investigated the structure, ionic conductivity, and performance in battery assembly of the (1-x) $Li_7P_2S_8I \cdot x$ (TMAI, TEAI, TPAI, and TBAI) (x = 0, 0.05, 0.1, and 0.2) (molar ratio) series. By introducing different types of tetraalkylammonium ions, I aim to significantly improve the mechanical flexibility and morphological adaptability of the electrolyte while maintaining high ionic conductivity.

The prepared electrolytes were thoroughly analyzed using various characterization techniques, including:

- X-ray Diffraction (XRD): To determine the crystal phase structure of the samples, confirming the crystallinity and phase purity of the materials.

- Scanning Electron Microscopy (SEM) and Energy Dispersive Spectroscopy (EDS): To observe the microstructure and elemental distribution of the samples, assessing material uniformity and structural features.
- Electrochemical Impedance Spectroscopy (EIS) and DC Polarization Tests: To measure the ionic conductivity and electrochemical stability of the electrolyte.
- Thermogravimetric-Differential Thermal Analysis (TG-DTA): To evaluate the thermal stability of the materials, identifying decomposition temperatures and phase transitions.
- Indentation Testing: To assess the mechanical properties of the materials and verify their ability to accommodate the volume changes of silicon electrodes.
- Assembly and Testing of All-Solid-State Batteries: The prepared electrolytes were assembled with silicon anode materials into all-solid-state batteries. To mitigate moisture sensitivity issues in both the electrolyte and electrode materials, the assembly process was conducted in a dry argon environment. The assembled all-solid-state batteries underwent charge-discharge cycling tests under constant current conditions to evaluate their cycling performance and capacity retention.

By developing a novel organic-inorganic hybrid sulfide solid electrolyte and systematically studying its physical and electrochemical properties, this study aims to provide an innovative solution for improving the energy density, cycle life, and safety of all-solid-state batteries.

Chapter 2 Experimental Section

2.1 Experimental Materials and Sample Preparation

A series of sulfide solid electrolyte samples, specifically (1-x) $Li_7P_2S_8I$ · x (TMAI, TEAI, TPAI, TBAI) with x = 0, 0.05, 0.1, and 0.2 (molar ratio), were synthesized in this study. All raw materials were of high-purity chemical grade to ensure reliability and reproducibility of results. The raw materials included lithium sulfide (Li_2S, Mitsuwa Chemical, 99.9%), phosphorus pentasulfide (P_2S_5, Aldrich, 99%), lithium iodide (LiI, Sigma Aldrich, 99.9%), tetramethylammonium iodide (TMAI, Sigma Aldrich, 99%), tetraethylammonium iodide (TEAI, Sigma Aldrich, 98%), tripropylammonium iodide (TPAI, Tokyo Chemical Industry, >98%), and tetrabutylammonium iodide (TBAI, Tokyo Chemical Industry, >98%).

Each raw material was weighed according to predetermined molar ratios to ensure strict stoichiometric control. Individual raw materials were manually ground for 15 minutes to increase surface area and improve reaction kinetics. The pre-ground raw materials were then mixed and placed in a 45 mL zirconia milling jar, with 90 grams of 4 mm zirconia balls as the grinding medium. The mixture was ball-milled in a high-energy planetary ball mill at 510 rpm for 24 hours to ensure thorough mixing and promote solid-state reactions. The entire ball-milling process was conducted under an inert argon atmosphere to prevent the sample from exposure to moisture and oxygen, avoiding irreversible oxidation or hydrolysis reactions.

2.2 Structural Characterization

The structure of the samples was characterized using X-ray diffraction (XRD) and Raman spectroscopy to confirm phase composition, crystal structure, and the effects of doping on the microstructure. XRD measurements were conducted with a Rigaku Miniflex 600 X-ray diffractometer using Cu Kα radiation over a range of 10° to 40° (2θ) with a step size of 0.02°, using Si powder as an internal reference.

Raman spectra were obtained with a Horiba XploRA Raman microscope, using an excitation wavelength of 532 nm, with a measurement range from 200 to 4000 cm^{-1} and a spectral resolution of 1 cm^{-1}. Raman analysis provided additional insights into the effects of different dopants on chemical bonding and local structural properties.

2.3 Electrochemical Performance Testing

The ionic conductivity of the pressed samples was measured to evaluate their potential in solid-state batteries. 100 mg of the solid electrolyte powder was pressed at 360 MPa for 5 minutes at room temperature, forming a 10 mm diameter pellet. For ionic conductivity measurements, two 10 mm diameter stainless steel (SS) plates were used as current collectors, and electrochemical impedance spectroscopy (EIS) was conducted with a Solartron SI 1260 impedance analyzer over a frequency range of 1 MHz to 1 Hz with a 10 mV amplitude. A 65 MPa pressure was applied on both sides of the sample during measurement to simulate the working conditions within solid-state batteries.

Electronic conductivity was assessed by DC polarization measurements. Multiple voltages (0.1 V, -0.1 V, 0.2 V, -0.2 V, 0.3 V, -0.3 V) were applied to the SUS/(1-x) $Li_7P_2S_8I$ · x TMAI (x = 0, 0.2)/SUS cell, recording the current response to evaluate the electrolyte's electronic insulation

properties. The sample preparation and equipment used for this test were identical to those for ionic conductivity measurements to ensure consistency.

2.4 Thermal Stability Characterization

The thermal stability of the samples was assessed using thermogravimetric-differential thermal analysis (TG-DTA) on a Thermo plus EV02 analyzer under an argon atmosphere with a heating rate of 10°C per minute. This test measured the thermogravimetric and thermal difference signals of the samples to determine their decomposition and crystallization temperatures, providing insights into the materials' stability at elevated temperatures.

2.5 Indentation Testing

To assess the mechanical properties, especially flexibility and deformation resistance, indentation testing was performed. Samples for indentation were prepared in an argon-filled glove box and pressed at 330 MPa for 10 minutes, forming a 10 mm diameter pellet with a thickness of approximately 1.5 mm. Samples were fixed on a superhard alloy sample holder and immersed in KF-968-100CS silicone oil (New Japan Chemical Co., Ltd.) to minimize friction during indentation.

Indentation testing was conducted on an RTF-1250 materials tester (A&D Systems) outside the glove box. The maximum load was set to 50 N, ensuring sufficient indentation depth without exceeding one-tenth of the sample thickness. The spherical indenter had a radius of Φ12 mm or Φ1.2 mm, with an indentation speed of 0.03 mm/min. The load-depth (P-h) curve was recorded, and the elastic modulus was calculated according to standard procedures to evaluate mechanical performance and deformation resistance.

2.6 SEM-EDS Analysis

The morphology and elemental distribution of the samples were analyzed using scanning electron microscopy (SEM) and energy dispersive spectroscopy (EDS). A JSM-IT500 SEM with an attached EDS spectrometer and a 532 nm laser was used to capture images of the morphology and elemental distribution of sulfide solid electrolyte particles. Samples were placed in a glove box under a nitrogen atmosphere at a dew point of -20°C before SEM observation to avoid moisture exposure.

2.7 Assembly and Testing of All-Solid-State Batteries

The prepared solid electrolytes were assembled with silicon anode materials into all-solid-state batteries to evaluate their electrochemical performance and cycling stability. The composite anode was prepared by mixing conductive silicon (ELKEM), (1-x) $Li_7P_2S_8I$ · x TMAI (x = 0, 0.05, 0.1, 0.2), and acetylene black (AB) in a weight ratio of 60:40:6. Amorphous $75Li_2S{\cdot}25P_2S_5$ (mol%) and Li-In alloy were used as separator and counter electrode, respectively. The electrolyte powder (100 mg) was pressed under 360 MPa for 5 minutes, followed by pressing lithium foil on both sides of the electrolyte pellet at 100 MPa for 2 minutes to ensure good contact between electrodes and electrolytes.

The charge-discharge tests were conducted at a constant current (CC) mode using a Scribner Associates 580 battery testing system at 25°C. The initial discharge cycle was conducted at a low current of C/30 to ensure full electrode activation, with subsequent cycles at 0.1C. The cutoff voltage at room temperature was set between -0.62 and 0.88 V. The specific battery configuration is illustrated in Figure 2.1.

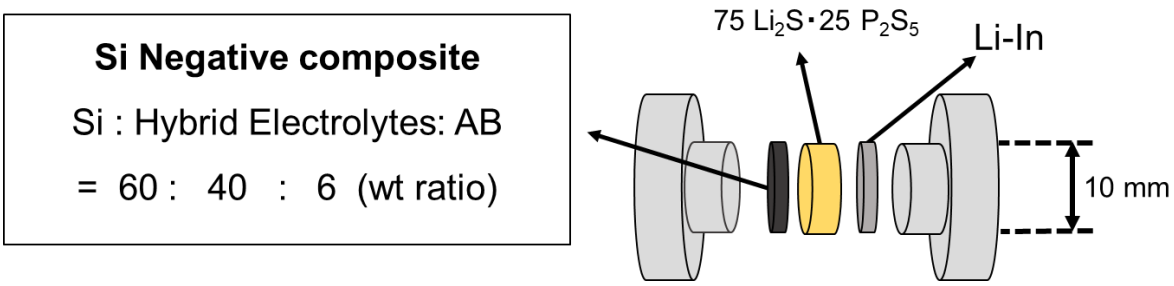

Figure 2.1. Battery Configuration

Through the above series of precise preparation and characterization steps, we systematically evaluated the structure, thermal properties, electrochemical performance, and mechanical properties of the developed organic-inorganic hybrid sulfide solid electrolyte. These experimental data provide a scientific basis for further improving the performance of all-solid-state lithium batteries and lay a foundation for exploring the feasibility of novel solid electrolyte materials in practical battery applications.

Chapter 3 Preparation and Evaluation of (1-x) $Li_7P_2S_8I$ · x TMAI (x = 0, 0.05, 0.1, 0.2) Inorganic-Organic Hybrid Electrolytes

3.1 Introduction

All-solid-state lithium batteries have attracted widespread attention in recent years due to their advantages in safety, energy density, and power density. In the development of all-solid-state batteries, sulfide-based solid electrolytes have become a key research focus due to their high ionic conductivity and good deformability.[33-36] As early as the early 2020s, sulfide solid electrolytes were applied in all-solid-state battery research for electric vehicles because these electrolyte particles can be pressed together, facilitating ion transport across grain boundaries.[21, 37] However, how to further enhance their energy density remains an unresolved issue. To achieve high energy density, researchers have explored all-solid-state batteries using high-capacity anode materials such as lithium metal and silicon. Nonetheless, the stability of solid electrolytes with lithium metal remains a key challenge.[38, 39] Sulfide solid electrolytes containing LiI (such as Li_4PS_4I, $Li_7P_2S_8I$, and LiI-Li_2S-P_2S_5 glass and glass-ceramics) have become a research focus for lithium metal anode-based all-solid-state batteries due to their interfacial stability with lithium metal and their ability to effectively suppress lithium dendrite formation.[40-46]

Using silicon as the anode material in all-solid-state lithium batteries, with its high theoretical capacity (>4200 mAh g^{-1}), is expected to further enhance the energy density of the batteries.[47] However, the significant volume expansion and contraction of silicon during charge and discharge lead to structural degradation of the electrode and electrolyte, severely affecting cycling performance.[47] Therefore, developing a sulfide glass or crystalline electrolyte that can mitigate

electrode cracking caused by silicon's volume changes is key to achieving high-energy-density all-solid-state batteries.

In recent years, introducing new components into electrolyte materials has proven to be an effective approach for developing novel sulfide glass electrolytes.[48-50] By adding various components, researchers have successfully designed novel electrolyte systems, with doping and substitution strategies significantly enhancing sulfide conductivity to the range of 10^{-3} - 10^{-2} S cm^{-1}.[27, 28]。

Research by J. Kawamura et al. has shown that introducing organic cations, such as tetraethylammonium iodide (TEAI) and tetramethylammonium iodide (TMAI), into AgI-CsI glass can create highly conductive systems.[32] Studies have found that the AgI-TMAI system achieves an ionic conductivity of up to 10^{-2} S cm^{-1} at room temperature. This is because tetraalkylammonium ions do not significantly attract surrounding silver cations, thereby forming pathways in the glass matrix that facilitate silver ion conduction. This finding offers a new approach for developing highly conductive inorganic-organic hybrid solid electrolytes.

Building on the above approach, this chapter develops an inorganic-organic hybrid solid electrolyte by introducing organic materials into an inorganic sulfide electrolyte. A novel glass solid electrolyte, $[N(CH_3)_4]I$ (TMAI)-LiI-Li_2S-P_2S_5, was prepared by doping tetramethylammonium iodide into a sulfide-based solid electrolyte. Figure 3.1 shows the structural model of the electrolyte, where the larger volume of organic cations provides pathways for lithium-ion conduction. Wu et al. previously synthesized $Li_7P_2S_8I$ glass-ceramics with enhanced ionic conductivity by incorporating LiI into Li_3PS_4 in a 2:1 molar ratio through mechanical milling, demonstrating improved dendrite suppression and electrochemical stability.[42] Therefore, in this study, I prepared the inorganic-organic hybrid electrolyte (1-x) $Li_7P_2S_8I$ · x TMAI (x = 0, 0.05, 0.1,

0.2, molar ratio) by doping TMAI into $Li_7P_2S_8I$ through mechanical milling. Experimental results showed that with increasing amounts of TMAI doping, the conductivity of the samples remained stable. The main reason for selecting the $Li_7P_2S_8I$ system is its high ionic conductivity and amorphous structure. Unlike crystalline materials such as Li_7PS_6, this amorphous structure facilitates doping and offers greater design flexibility.[51] Additionally, compared to amorphous Li_3PS_4, $Li_7P_2S_8I$ contains a LiI component, which greatly enhances its stability with lithium metal. I hypothesize that introducing TMAI not only improves the flexibility of the sulfide electrolyte but also significantly enhances its fracture toughness and plasticity. These improvements enable the electrolyte to effectively absorb and withstand various physical stress encountered during battery operation, including compression, tension, or torsion. More importantly, the enhanced mechanical properties strengthen the electrolyte's stability, allowing it to resist deformation over multiple charge-discharge cycles without fracturing. This robust mechanical stability is crucial for preventing internal structural damage, thereby ensuring stable performance and improved safety throughout the battery's lifecycle.

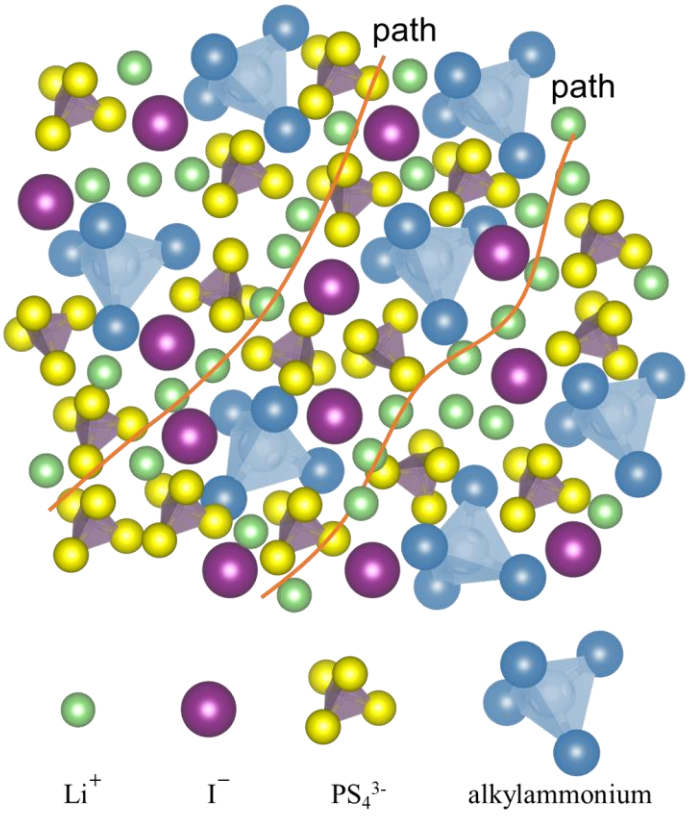

Figure 3.1. Structure diagram of electrolyte

3.2 Results and Discussion

XRD patterns of the prepared samples are shown in **Figure 3.2**. The XRD patterns of the samples show halo with Si added as the angle reference, and thus the prepared materials were found to be amorphous. The SEM-EDS images of (1-x) $Li_7P_2S_8I \cdot x$ TMAI (x = 0, 0.2) samples (Figure 3.3) showed no significant difference before and after TMAI doping, and P, S, and I are homogenously distributed, meaning that no aggregation of TMAI was found. The particle size was about 1 μm**.**

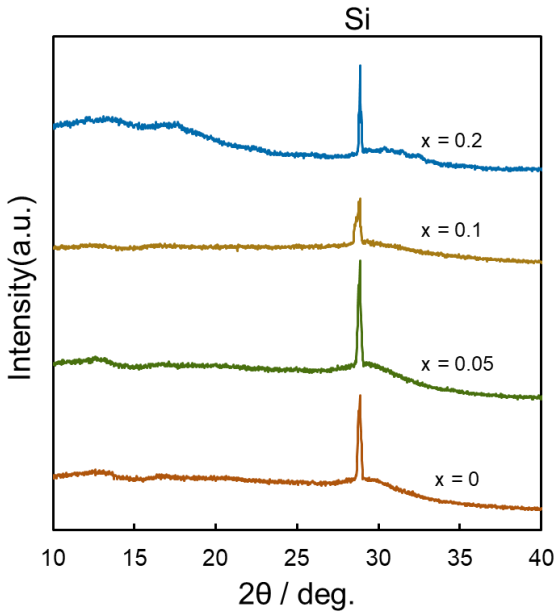

Figure 3.2. XRD patterns of the obtained (1-x) $Li_7P_2S_8I \cdot x$ TMAI (x = 0, 0.05, 0.1, 0.2) samples. Si was added as the angle reference.

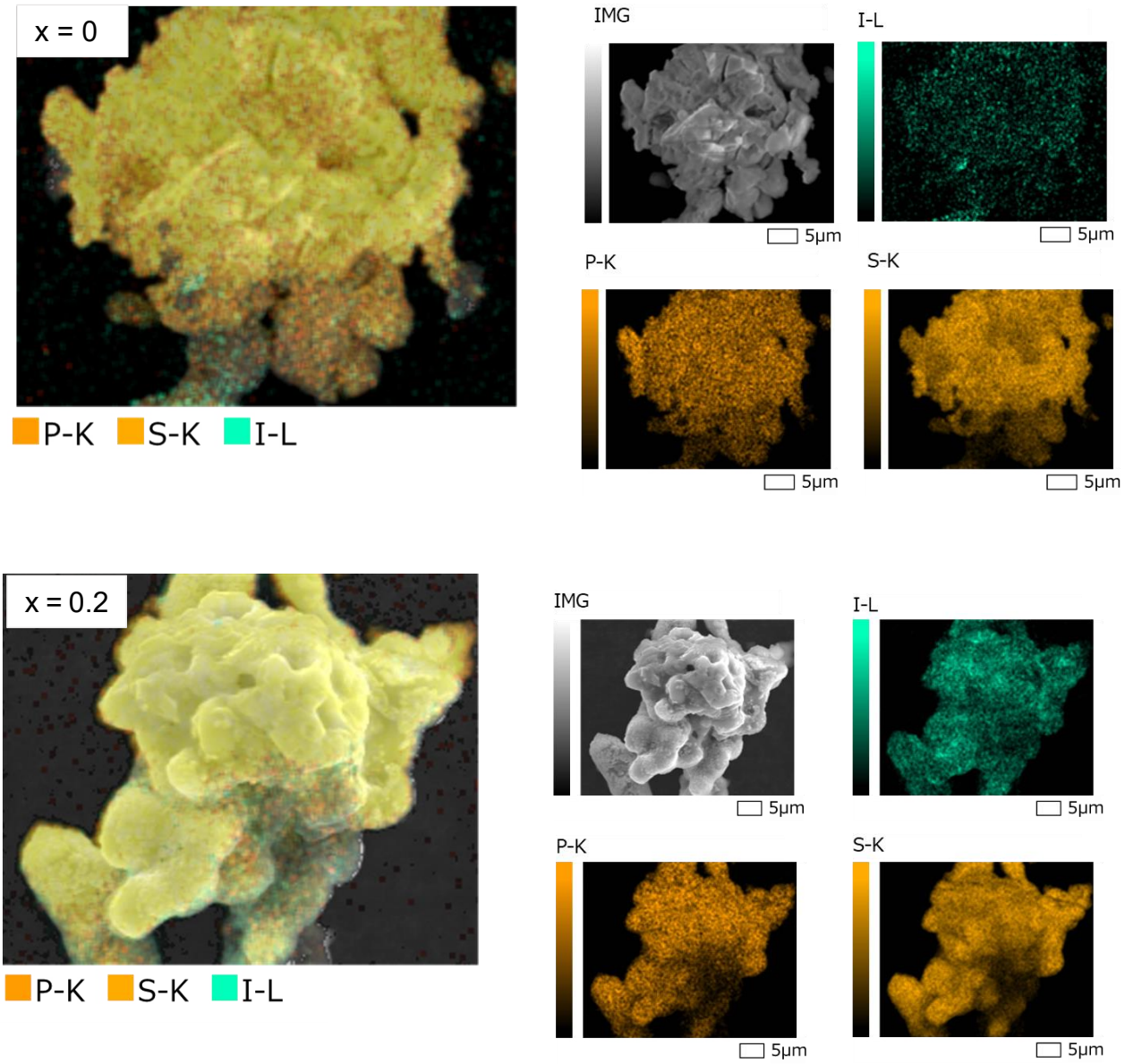

Figure 3.3. The SEM-EDS images of (1-x) $Li_7P_2S_8I \cdot x$ TMAI (x = 0, 0.2) after ball milling.

The Nyquist plots of the samples at room temperature are shown in **Figure 3.4(a)**, and the ionic conductivity of the prepared samples are shown in **Table 3.1**. The temperature dependence of the ionic conductivity of these samples are shown in **Figure 3.4(b)**, and the activation energy ($E_{a.}$) was calculated from the slope of this temperature dependence. The specific values are shown in **Table 3.2**. The composition dependence of the activation energy and conductivity are plotted in **Figure 3.5.**

As shown in **Figure 3.4 and Table 3.1,** the total ionic conductivity of the undoped sample was 3.8×10^{-4} S cm^{-1} at room temperature, and the doping of TMAI is found to have no significant decrease in total conductivity, which remains at the same level as before the doping. At the same time, as the TMAI doping content increased, the bulk conductivity slightly increased, which demonstrated that the doping of TMAI does facilitate the conduction of lithium ions. However, the total ion conductivity decreased because the TMAI doping affects the interfacial contact and increases the grain boundary resistance. As shown in Figure 3.5, the activation energies do not differ much by the addition of TMAI and are relatively low.

In addition, the electronic conductivity of both x = 0 and x = 0.2 samples were measured to be approximately 2.0×10^{-7} S cm^{-1} as shown in **Figure 3.6**, indicating that the TMAI doping does not change the electronic conductivity of the $Li_7P_2S_8I$. Meanwhile, both the Li / $Li_7P_2S_8I$ / Li symmetrical cell (x=0) and the Li / (1-x) $Li_7P_2S_8I$ ·xTMAI (x=0.2) /Li symmetrical cell can realize stable lithium plating/stripping for about 60 h at room temperature (**Figure 3.7**).

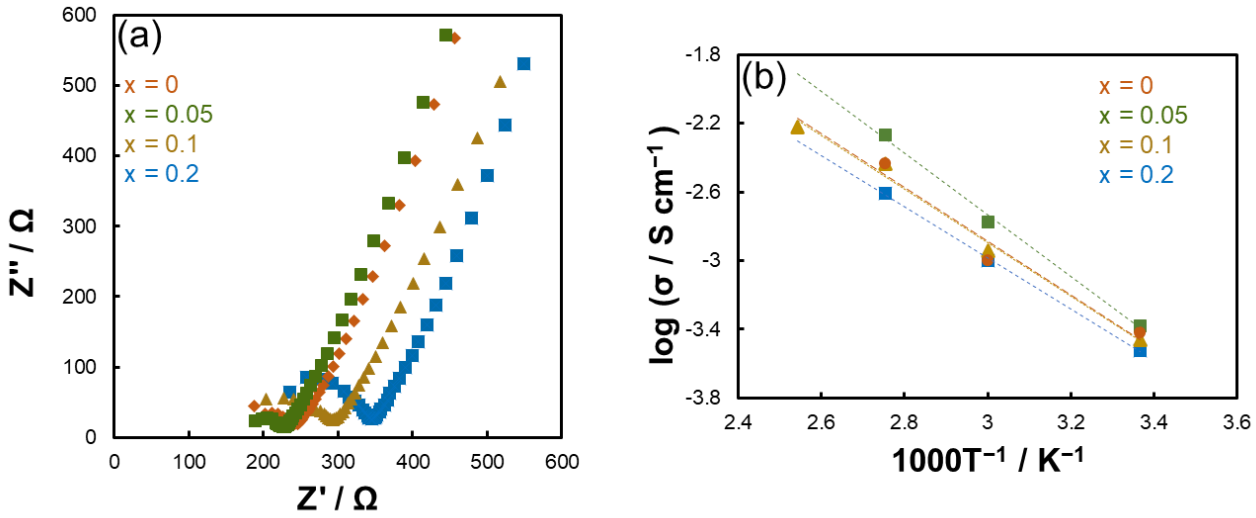

Figure 3.4. (a) The Nyquist plots of (1-x) $Li_7P_2S_8I \cdot x$ TMAI (x = 0, 0.05, 0.1, 0.2).

(b) Arrhenius plots of (1-x) $Li_7P_2S_8I \cdot x$ TMAI (x = 0, 0.05, 0.1, 0.2).

Table 3.1. Comparison of ionic conductivity of samples.

Sample		Bulk Conductivity / S cm^{-1}	Total Conductivity / S cm^{-1}
$Li_7P_2S_8I$	25℃	5.0×10^{-4}	3.8×10^{-4}
0.95 $Li_7P_2S_8I \cdot$ 0.05 TMAI	25℃	6.3×10^{-4}	4.2×10^{-4}
0.9 $Li_7P_2S_8I \cdot$ 0.1TMAI	25℃	7.3×10^{-4}	3.5×10^{-4}
0.8 $Li_7P_2S_8I \cdot$ 0.2 TMAI	25℃	7.8×10^{-4}	3.0×10^{-4}

Table 3.2. Activation energy of samples.

Sample	Activation Energy / kJ mol^{-1}
$Li_7P_2S_8I$	13.0
0.95 $Li_7P_2S_8I$ · 0.05 TMAI	14.9
0.9 $Li_7P_2S_8I$ · 0.1 TMAI	12.9
0.8 $Li_7P_2S_8I$ · 0.2 TMAI	12.4

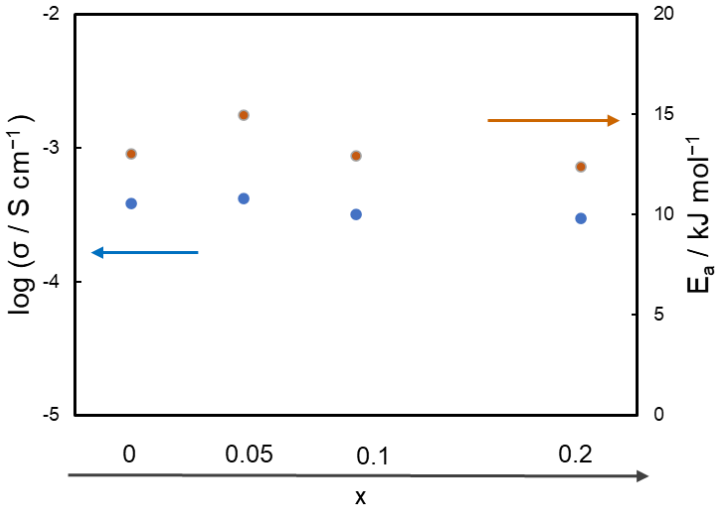

Figure 3.5. Activation energy and Arrhenius plots trend of (1-x) $Li_7P_2S_8I$ · x TMAI (x = 0, 0.05, 0.1, 0.2)

(1) x = 0

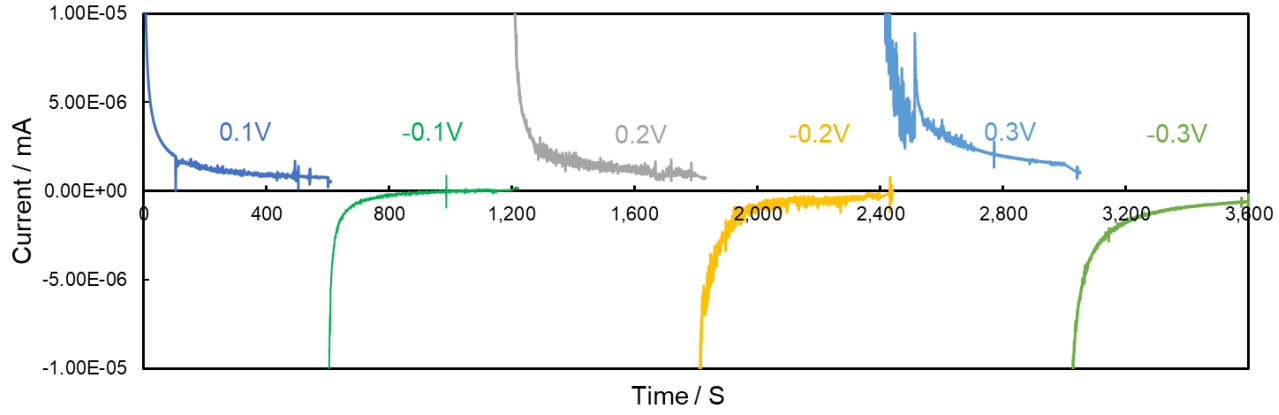

(2) x = 0.2

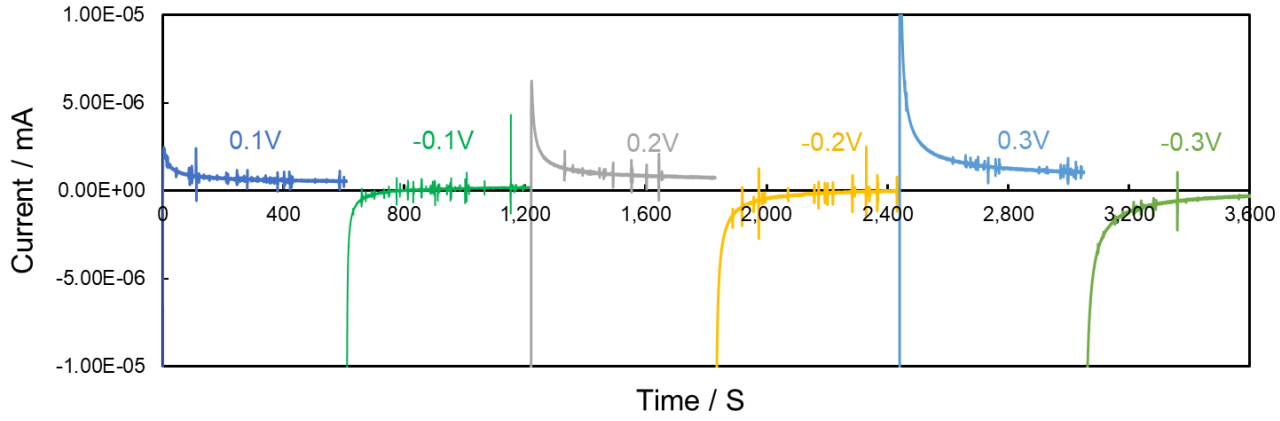

Figure 3.6. Direct-current polarization curves of SUS / (1-x) $Li_7P_2S_8I$·xTMAI (x = 0, 0.2) /SUS cells.

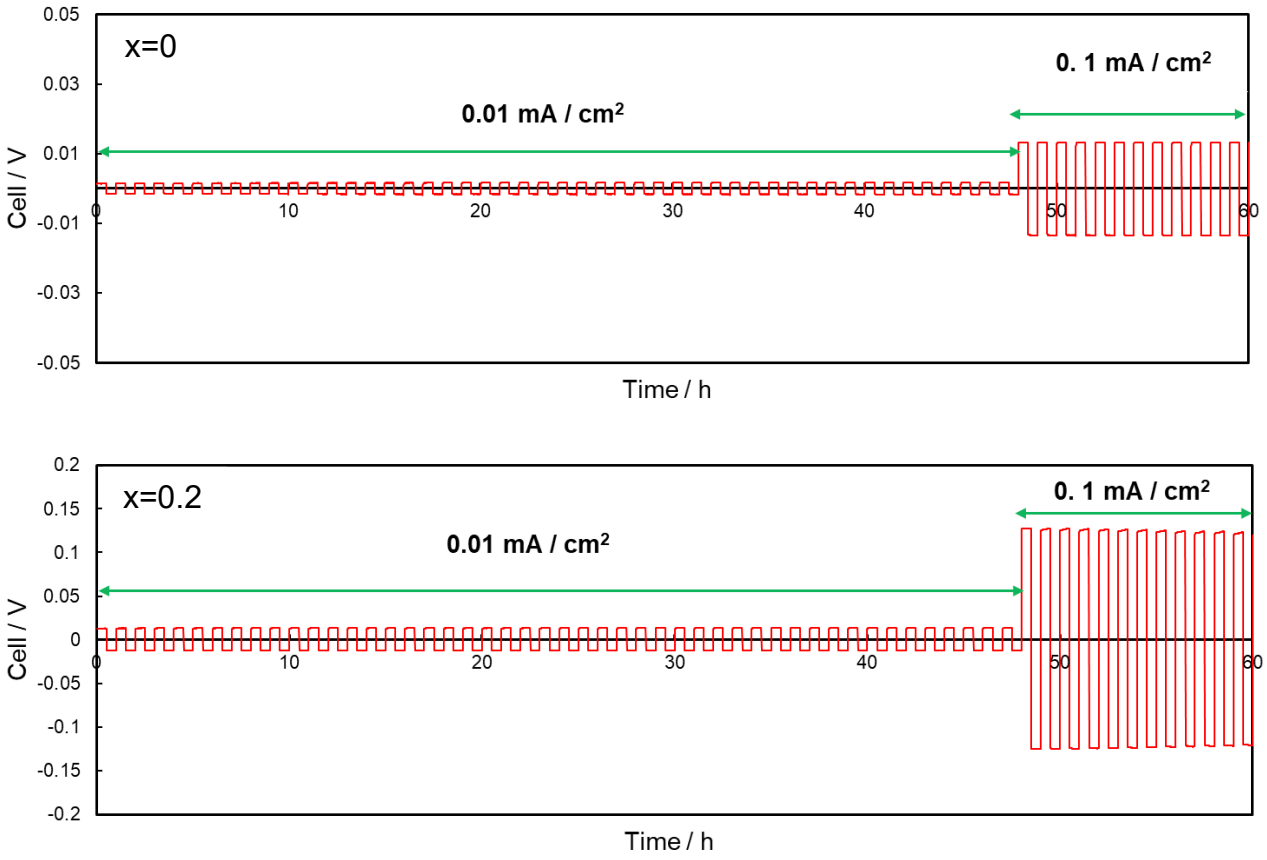

Figure 3.7. Cycling performances of Li / (1-x) $Li_7P_2S_8I$ ·xTMAI / Li symmetrical cells of x = 0 and x = 0.2 samples.

All samples were heat treated at 120°C for 2 hours to check their thermal stability. XRD results are shown in **Figure 3.8**. It was found that the samples (x = 0, 0.05, 0.1) remained in their original amorphous state with no crystallization, whereas the sample of x = 0.2 showed some peaks which were assigned as $Li_7P_2S_8I$ [52] and TMAI phase. The observation of TMAI peak after heat treatment indicates that the TMAI was dispersed in the particles after ball milling, but then phase separation occurred after heating at 120℃ for 2h.

The TG-DTA curves of the samples are shown in **Figure 3.9(a)**. The small exothermic peaks are observed in all samples, and these peaks are assigned to the crystallization from the amorphous state. The crystallization temperatures for all samples are between approximately 150-200°C. **Figure 3.9(b)** shows the composition dependence of the crystallization temperature. This figure reveals that the crystallization temperature slightly decreases with an increase in TMAI doping amount, showing that TMA cations are homogenously distributed in the glassy matrix. The decrease in crystallization temperature can be because the large molecules of TMAI make the structure lose, molecular movement becomes easier, and the viscosity is reduced, which indicates that nucleation can be accelerated by the addition of TMAI.

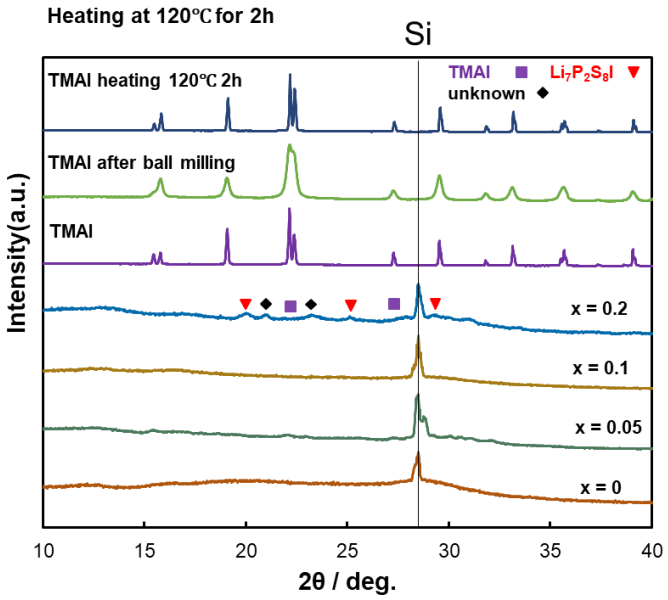

Figure 3.8. XRD patterns of heat-treated (1-x) $Li_7P_2S_8I$ · x TMAI (x = 0, 0.05, 0.1, 0.2) and TMAI.

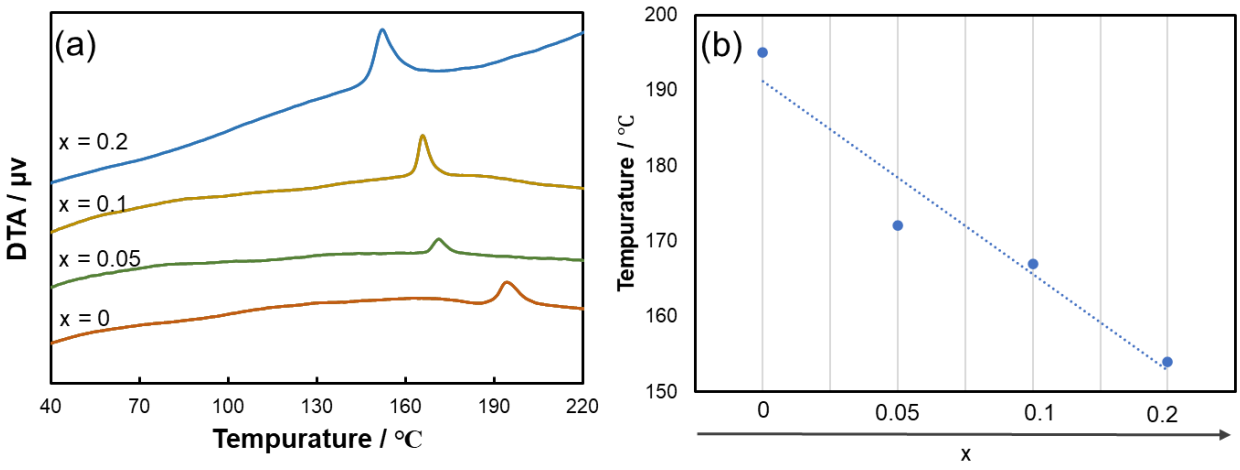

Figure 3.9. (a) TG-DTA plots of all samples.

(b) Crystallization temperature trends for all samples.

3.3 Chapter Conclusion

In this section, the influence of TMAI doping on the ionic and electronic conductivity of (1-x) $Li_7P_2S_8I \cdot x$ TMAI electrolytes was studied. The results show that while TMAI doping slightly increased the bulk conductivity, the overall ionic conductivity remained stable with no significant decrease. However, the doping slightly increased the grain boundary resistance, leading to a minor reduction in total ionic conductivity. Importantly, the TMAI doping did not impact the electronic conductivity of the electrolyte, ensuring its suitability for lithium-ion conduction without compromising electronic insulation.

The symmetric cells demonstrated stable lithium plating/stripping performance, confirming that the (1-x) $Li_7P_2S_8I \cdot x$ TMAI electrolytes can maintain good interfacial stability with lithium metal over extended cycles. These findings indicate that TMAI-doped $Li_7P_2S_8I$ electrolytes have promising properties for practical application in high-energy-density solid-state lithium batteries, balancing high ionic conductivity with mechanical stability and interfacial compatibility.

Based on the current research findings, the effects of other dopants (TEAI, TPAI, TBAI) on the performance of (1-x) $Li_7P_2S_8I$ electrolytes were further studied in the next section. The specific impacts of these dopants on electrolyte structural stability, ionic conductivity, and thermal properties were discussed.

Chapter 4 Preparation and Evaluation of (1-x) $Li_7P_2S_8I$ · x (TMAI, TEAI, TPAI, TBAI) (x = 0, 0.05, 0.1, 0.2) Inorganic-Organic Hybrid Electrolytes

4.1 Introduction

As a core component of electric vehicles and portable electronic devices, solid electrolytes must exhibit excellent ionic conductivity and sufficient mechanical stability to withstand the physical stresses encountered during battery operation.[53-55] During the charge and discharge processes, lithium dendrites may form on the anode and penetrate the solid electrolyte, leading to risks of short circuits, overheating, or even explosions. [11] Therefore, electrolytes are required to have high fracture toughness and ductility, as well as good deformation recovery capability, moderate deformation resistance, and low hardness. These properties work together to effectively prevent crack formation and propagation, thereby avoiding lithium dendrite penetration. Additionally, maintaining good contact between the electrolyte and electrodes is essential for efficient ion transport. Under stress, deformation or fracture of the electrolyte can lead to poor contact, affecting battery performance and reducing battery lifespan.[8] For example, silicon-based anode materials, though possessing high theoretical energy density, undergo significant volume expansion during charge and discharge cycles, which can damage the electrode structure and shorten battery life.[56-59]

In Chapter 3, I found that introducing tetramethylammonium iodide (TMAI) into the $Li_7P_2S_8I$ sulfide solid electrolyte lowered the glass transition temperature without compromising conductivity, suggesting a reduction in material viscosity, which facilitates improved flexibility and processability. [60] Sulfide-based solid electrolytes offer significant advantages in ionic conductivity and mechanical performance compared to conventional oxide-based solid

electrolytes, particularly due to their lower elastic modulus, which allows better accommodation of volume changes during charge-discharge cycles. This reduces the risk of material fracture from stress concentration, enhancing the operational stability and safety of the battery. [61-63] This chapter continues to develop innovative, softer inorganic-organic hybrid sulfide electrolytes.

This chapter explores the effects of incorporating various organic components, such as tetraethylammonium iodide (TEAI), tripropylammonium iodide (TPAI), and tetrabutylammonium iodide (TBAI), into the $Li_7P_2S_8I$ electrolyte. Multiple characterization techniques were employed to analyze these novel inorganic-organic hybrid sulfide electrolytes, including X-ray diffraction (XRD) for examining the crystalline structure of materials, differential thermal analysis (DTA) to assess thermal stability, and ionic conductivity measurements to determine electrochemical performance. Through this systematic investigation, the aim is to overcome the limitations of traditional sulfide electrolytes in mechanical stability, thereby developing new electrolyte materials with superior mechanical and electrochemical properties.

4.2 Results and Discussion

As illustrated in **Figure 4.1**, the molecular structures of these doping agents show a progressive increase in the length of the alkyl chains, ranging from four methyl groups in TMAI to four butyl groups in TBAI, presenting incremental structural characteristics. The molecular structure of each doping agent includes alkyl chains of varying lengths, which are expected to influence the capacity of the electrolyte and improve its physical and chemical properties.

Subsequently, the electrolytes were prepared by mixing Li_2S, P_2S_5, and LiI with different proportions of the doping agents TMAI, TEAI, TPAI, and TBAI using mechanical ball milling. **Figure 4.2** shows the XRD patterns of the TMAI, TEAI, TPAI, and TBAI samples at different concentrations (x = 0, 0.05, 0.1, and 0.2). XRD analysis revealed that after the ball-milling process, all samples showed halos and largely preserved an amorphous configuration, with Si added as the angle reference.

a. TMAI : Tetramethylammonium iodide $(CH_3)_4N^+I^-$

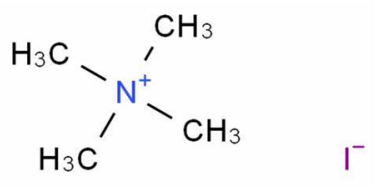

b. TEAI : Tetraethylammonium iodide $(C_2H_5)_4N^+I^-$

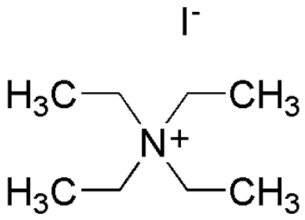

c. TPAI : Tetrapropylammonium iodide $(C_3H_7)_4N^+I^-$

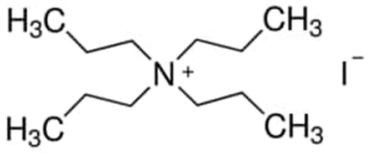

d. TBAI : Tetrabutylammonium iodide $(C_4H_9)_4N^+I^-$

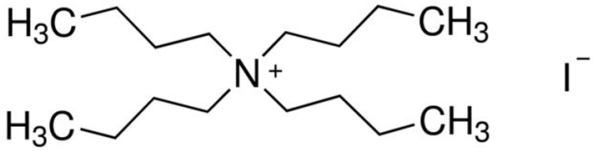

Figure 4.1. Structural Formula of TMAI, TEAI, TPAI, TBAI

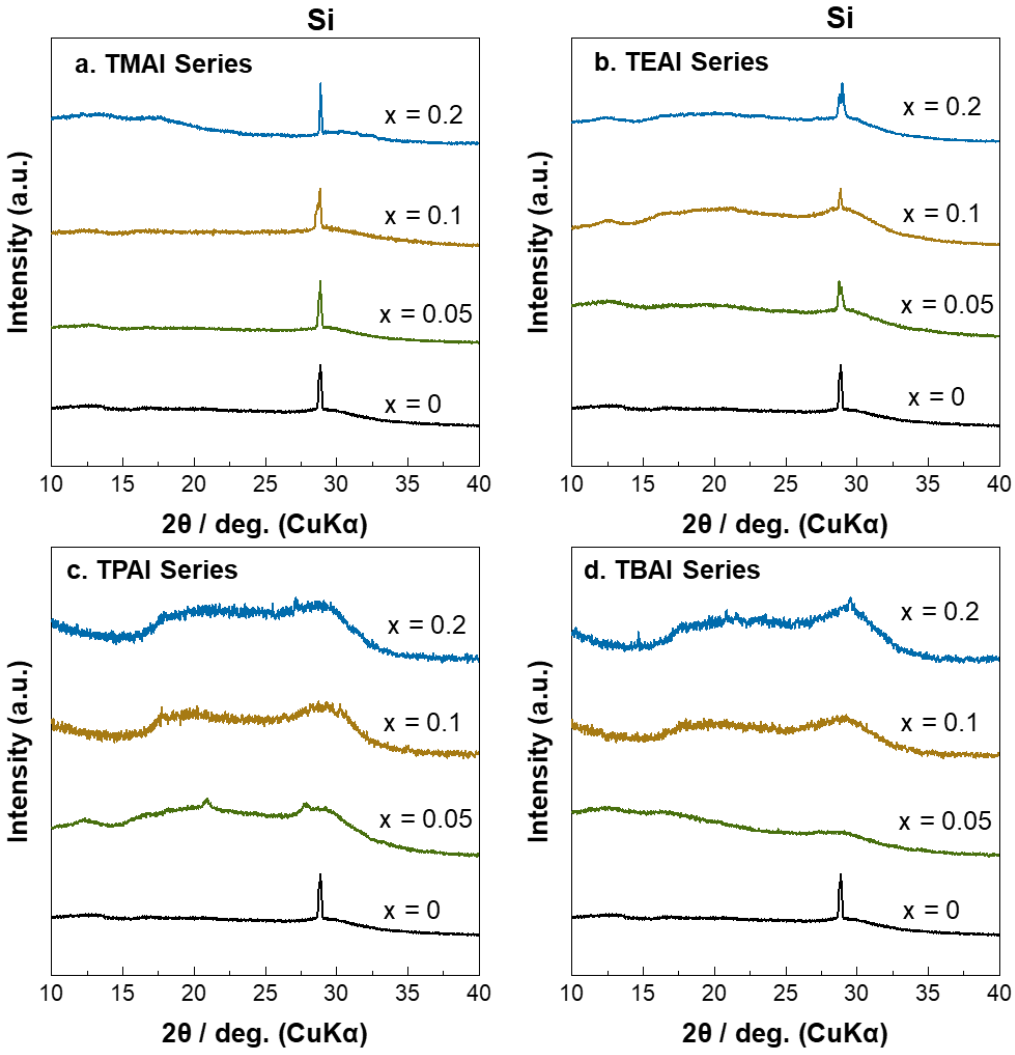

Figure 4.2. XRD Patterns of (1-x) $Li_7P_2S_8I \cdot x$ (TMAI, TEAI, TPAI, TBAI) (x = 0, 0.05, 0.1, 0.2). a) TMAI series, b) TEAI series, c) TPAI series, and d) TBAI series.

Figure 4.3 shows the DTA curves of the sulfide solid electrolytes at different doping levels (x = 0, 0.05, 0.1, and 0.2). In the TMAI, TEAI, TPAI, and TBAI series, all samples exhibited an exothermic peak during the heating process, indicating crystallization. **Table 4.1** lists the crystallization temperatures according to the dopant type.

In all series, the crystallization temperature decreases with increasing doping levels, which may be related to the alkyl chain length and structure of the doping agents. Our previous studies have shown that TMAI series after being treated at 120°C for 2 hours, the samples with x = 0.2 not only exhibited the known phases of $Li_7P_2S_8I$ and TMAI but also showed some unknown diffraction peaks. [18] These unknown peaks may indicate the formation of new phase structures under specific conditions, providing preliminary evidence of the hybrid characteristics of the material. I assume that the crystallization behavior in other systems should be like that of the TMAI system. The variation in crystallization temperature with composition suggests that the resulting electrolyte is not merely a mixture of sulfide solid electrolyte and tetraalkylammonium iodide, but a hybrid material with a dispersion of tetraalkylammonium iodide at the molecular level.

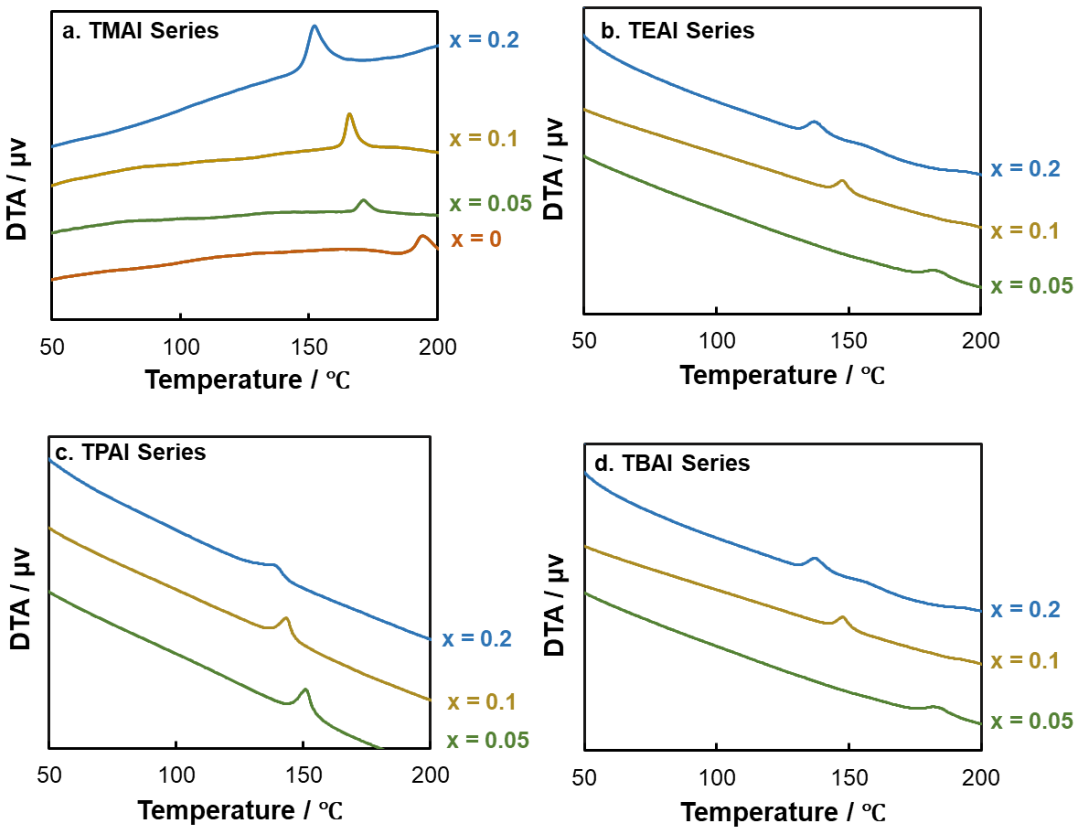

Figure 4.3. DTA Curves of (1-x) $Li_7P_2S_8I \cdot x$ (TMAI, TEAI, TPAI, TBAI) (x = 0, 0.05, 0.1, 0.2). a) TMAI series, b) TEAI series, c) TPAI series, and d) TBAI series.

Table 4.1. Crystallization temperature by dopant types (℃).

Samples	TMAI	TEAI	TPAI	TBAI
x = 0	195	195	195	195
x = 0.05	172	184	151	148
x = 0.1	167	148	144	145
x = 0.2	154	137	139	142

The Arrhenius plots (**Figure 4.4**) reveal the impact of different doping levels on the ionic conductivity of the sulfide solid electrolytes. The effects of different doping concentrations on the ionic conductivity (log σ) and activation energy (Ea) of sulfide solid electrolytes are depicted in **Figure 4.5**.

As shown in **Table 4.2** and **Figure 4.5**, the ionic conductivity decreases with increasing doping concentration for the TMAI, TEAI, TPAI, and TBAI series. The TEAI series shows a relatively smaller decrease in conductivity at x=0.05, with a more significant drop at x=0.1 and x=0.2. The TPAI series exhibited a pronounced decrease in conductivity as the doping concentration increased. For example, at x=0.1, the ionic conductivity of TPAI drops to 1.6×10^{-4} S cm^{-1}, and decreases to 7.8×10^{-5} S cm^{-1} at x=0.2. The TBAI series exhibited a significant reduction in conductivity at a lower doping level (x=0.05) and a corresponding increase in the activation energy, indicating that even a small amount of the long-chain dopant significantly affected the ion transport capabilities of the electrolyte. As the doping concentration increased to x=0.2, the ionic conductivity decreased further, and the activation energy continued to increase.

These results were further validated using Raman spectroscopy (**Figure 4.6**). The Raman spectra show that both the pure and TMAI-doped samples have peaks in the 400-500 cm^{-1} [64, 65] region, indicating the presence of only PS_4^{3-} units. However, the TMAI-doped sample also exhibits additional C-H bond peaks in the high-frequency region of 2800-3000 cm^{-1}, [66] confirming the incorporation of organic components.

In this study, from TMAI to TBAI, the increase in the length of the alkyl chain of the dopants had complex and varied effects on the ionic conductivity. As the alkyl chain length increased, there was a consistent trend of decreasing ionic conductivity and a corresponding increase in activation energy. Particularly in TBAI, although longer alkyl chains impede lithium-ion conduction by

increasing the volume occupied by non-conductive molecular parts, the looser structural arrangement seems to enhance lithium-ion migration efficiency by increasing the number of ion channels. Notably, this effect is especially pronounced at higher doping concentrations in TBAI (such as 0.1, 0.2), resulting in a slightly higher conductivity at these levels compared to TPAI. Although long-chain dopants may negatively affect the ion transport capabilities of electrolytes, they demonstrate potential advantages in terms of mechanical strength and long-term stability.

Table 4.2. Room temperature ionic conductivity (S cm^{-1}) for (1-x) $Li_7P_2S_8I \cdot x$ (TMAI, TEAI, TPAI, TBAI) (x = 0, 0.05, 0.1, 0.2)

Samples	TMAI	TEAI	TPAI	TBAI
x = 0	3.8×10^{-4}	3.8×10^{-4}	3.8×10^{-4}	3.8×10^{-4}
x = 0.05	4.2×10^{-4}	3.7×10^{-4}	3.8×10^{-4}	1.6×10^{-4}
x = 0.1	3.5×10^{-4}	2.8×10^{-4}	1.6×10^{-4}	1.8×10^{-4}
x = 0.2	3.0×10^{-4}	2.0×10^{-4}	7.8×10^{-5}	1.1×10^{-4}

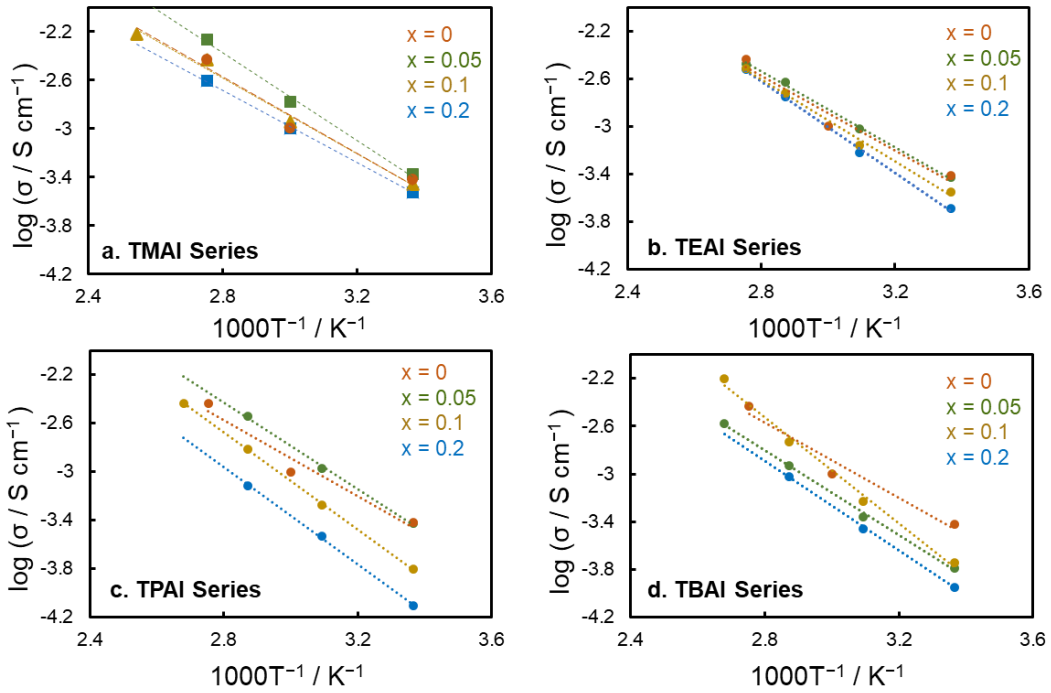

Figure 4.4. Arrhenius Plot of (1-x) $Li_7P_2S_8I \cdot x$ (TMAI, TEAI, TPAI, TBAI) (x = 0, 0.05, 0.1, 0.2). a) TMAI series, b) TEAI series, c) TPAI series, and d) TBAI series.

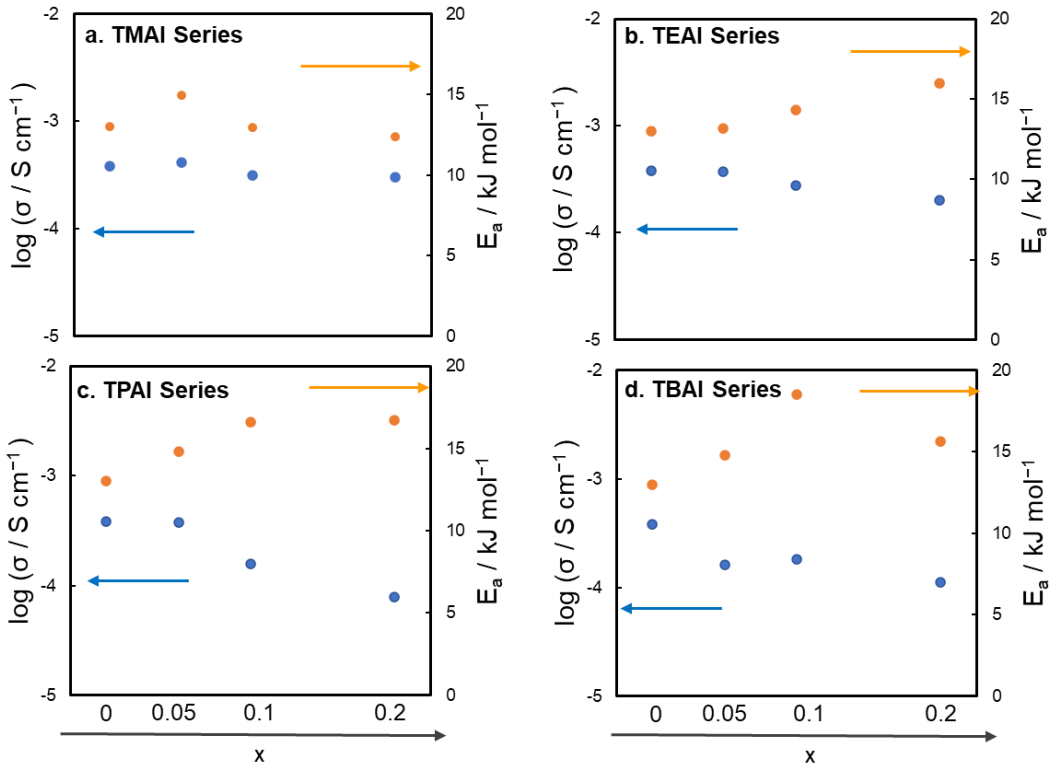

Figure 4.5. Composition dependence of (1-x) $Li_7P_2S_8I \cdot x$ (TMAI, TEAI, TPAI, TBAI) (x = 0, 0.05, 0.1, 0.2). a) TMAI series, b) TEAI series, c) TPAI series, and d) TBAI series.

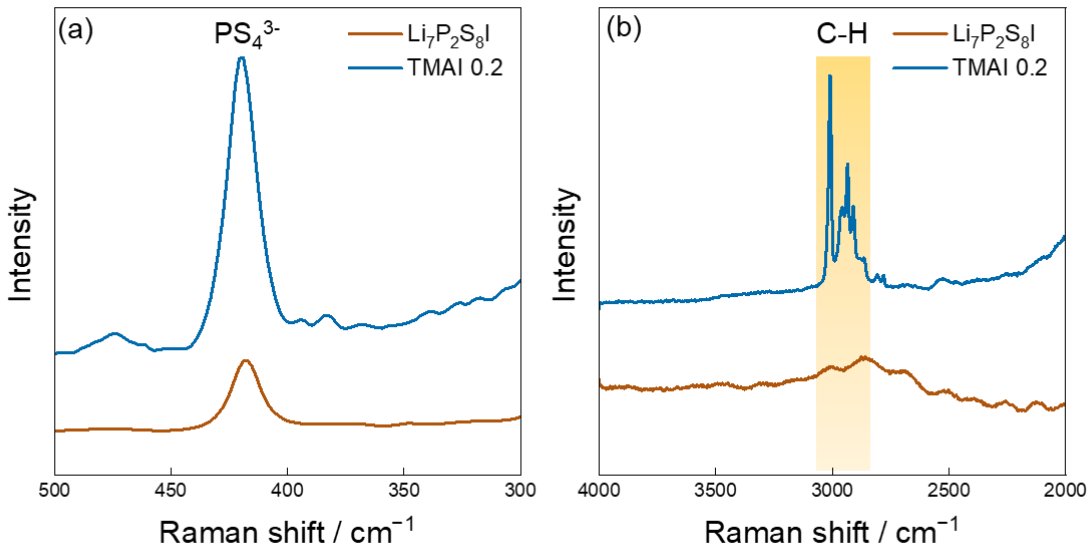

Figure 4.6. Raman spectra of samples.

4.3 Chapter Conclusion

This chapter systematically examined the effects of four tetraalkylammonium iodide dopants (TMAI, TEAI, TPAI, and TBAI) on the structure and electrochemical performance of Li_2S-P_2S_5-LiI-based solid electrolytes, with increasing alkyl chain lengths in the dopants. Results indicate that these dopants influence crystallization behavior and ionic conductivity. XRD patterns confirmed a mostly amorphous structure, while DTA analysis showed decreasing crystallization temperatures with higher doping levels, enhancing amorphous characteristics conducive to ion conductivity.

Ionic conductivity measurements revealed an overall decrease in conductivity with increased doping, with varying impacts across different dopants. Notably, the TBAI series exhibited nonlinear behavior, where longer alkyl chains initially hindered ion transport but improved at higher levels. Raman spectroscopy results supported these findings, showing the presence of both inorganic and organic units, emphasizing the composite nature of the electrolyte.

The interplay between alkyl chain length and electrolyte performance suggests the potential of these doped electrolytes in conjunction with silicon and lithium metal electrodes. These dopants' unique structures and ion pathways may improve compatibility with silicon electrodes. The enhanced amorphous structure and tailored conductivity may alleviate these issues, boosting battery stability and efficiency.

Future studies further combine these doped electrolytes with silicon and lithium metal electrodes to evaluate their potential to enhance energy density, cycling stability, and mechanical integrity in all-solid-state lithium batteries.

Chapter 5 Assembly and Evaluation of All-Solid-State Batteries

5.1 Introduction

In Chapters 3 and 4, a series of new inorganic-organic hybrid sulfide electrolytes was prepared, and their performance in all-solid-state lithium batteries was evaluated next. The effectiveness of the electrolyte layer is crucial in all-solid-state lithium batteries, as it must support efficient lithium ion conduction and maintain robust contact between the electrolyte and the electrodes. Previously, various organic cations such as TMAI, TEAI, TPAI, and TBAI were introduced, and the ionic conductivity and thermal stability of different $Li_7P_2S_8I$ electrolytes were characterized in detail. This chapter assesses the batteries' performance through testing, focusing on their cycle stability and capacity retention, as well as their ability to mitigate volume expansion in silicon-based electrodes during charging and discharging. The assembly and testing of all-solid-state lithium batteries based on these electrolytes are highlighted.

The electrolyte in all-solid-state batteries not only needs excellent ionic conductivity but also must accommodate the volume changes of the electrodes during charging and discharging, especially the notable expansion of silicon electrodes. The developed inorganic-organic hybrid sulfide electrolytes, by incorporating organic cations of varying molecular sizes, aim to enhance their compatibility and cycling performance with silicon electrodes. As the molecular weight of TMAI, TEAI, TPAI, and TBAI increases, the electrolyte structure becomes more porous and less viscous, potentially enabling better accommodation of volume changes in silicon electrodes, thus alleviating expansion issues and enhancing cycle stability.

This chapter details the assembly steps of all-solid-state lithium batteries and conducts cycle performance tests to evaluate their effectiveness in managing the volume expansion of silicon

electrodes. These experiments aim to further validate the performance of the newly developed inorganic-organic hybrid sulfide electrolytes in practical battery applications and assess their potential to advance all-solid-state battery technology.

5.2 Results and Discussion

5.2.1 Battery Results for $Li_7P_2S_8I$-TMAI

All solid-state lithium batteries using $Li_7P_2S_8I$-TMAI in the composite Si electrode were fabricated. The charge-discharge results are shown in **Figure 5.1**. The first discharge (Li insertion) was carried out at a low current to completely discharge the battery, which has a capacity of approximate 3000 mAh g^{-1}. The first charge (Li de-insertion) was then set to terminate in 2014 mAh g^{-1} to suppress the volume expansion and contraction of the Si. Subsequent discharge charges were all terminated in 2014 mAh g^{-1}. $Li_7P_2S_8I$ (x=0) and x= 0.05 samples showed a capacity of approximately 1200 mAh g^{-1} after 10 cycles, while x=0.1 sample showed a capacity of approximately 1400 mAh g^{-1} after 10 cycles, all showing some degree of capacity drop. However, the x=0.1, 0.2 sample maintained a capacity of 2014 mAh g^{-1} after 10 cycles without any drop, showing the best battery cycling performance in the present study. The addition of TMAI may change the mechanical properties of the solid electrolyte: TMAI addition should increase the deformability of the solid electrolyte, and thus the solid electrolyte can suppress the effect of the change of volume. The lowering of crystallization temperature (**Figure 4.3**) also supports the change of mechanical properties. Lowering of the crystallization temperature means lowering in the glass transition temperature, which should cause the lowering of the viscosity of the glass at room temperature. Thus, the deformability can be affected by the addition of TMAI, and the TMAI-doped sample showed better cycle performance. The Nyquist plots of the cells using (1-x)

$Li_7P_2S_8I \cdot x$ TMAI (x = 0, 0.2) before and after 10 cycles (**Figure 5.2**) showed that the x=0.2 sample had a smaller semicircle than the x=0 sample after 10 cycles, meaning that the x=0.2 sample had a smaller interfacial resistance. The smaller interfacial resistance should facilitate high cycling performance.

The SEM-EDS cross-sectional images of LixSi / $75Li_2S \cdot 25P_2S_5$ / Li-In cell, in which (1-x) $Li_7P_2S_8I$-xTMAI (x = 0, 0.2) was used in the electrode composite with Li_xSi, before and after 2 cycles at 0.1C are shown in **Figure 5.3 and 5.4**. Before cycling, the Si composite electrodes of both x=0 and x=0.2 samples were approximately 20 μm thick and had a dense structure. After two cycles, the thickness of the Si composite electrode of the sample with x=0 was about 50 μm, and that of the sample with x=0.2 was about 20 μm. This means that the TMAI-free Si negative electrode sample swelled, but the Si negative electrode composite containing TMAI with x=0.2 had almost no expansion. In addition, the structure of Si electrode composite containing TMAI with x=0.2 remained dense after two cycles, whereas the particles in the TMAI-free Si electrode composite split apart, and the electrode composite was no longer dense. This means that TMAI did suppress the volume expansion of Si electrode composite, and the addition of TMAI should prevent electrode cracking that may happen after cycling.

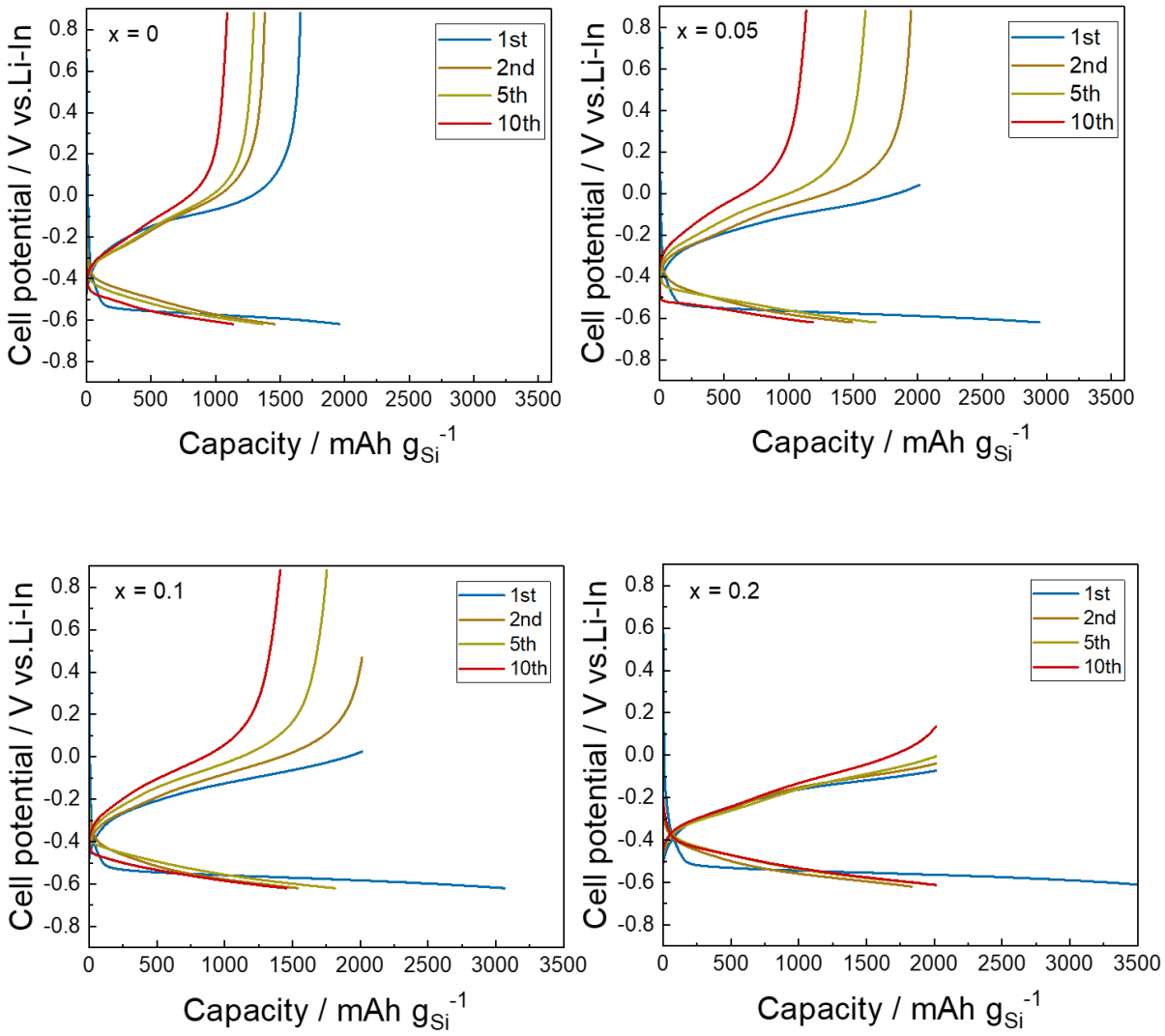

Figure 5.1. The charge-discharge curves of Li_xSi / $75Li_2S{\cdot}25P_2S_5$ / Li-In cells, in which (1-x) $Li_7P_2S_8I{\cdot}xTMAI$ (x = 0, 0.05, 0.1, 0.2) were used in the Li_xSi electrode composite.

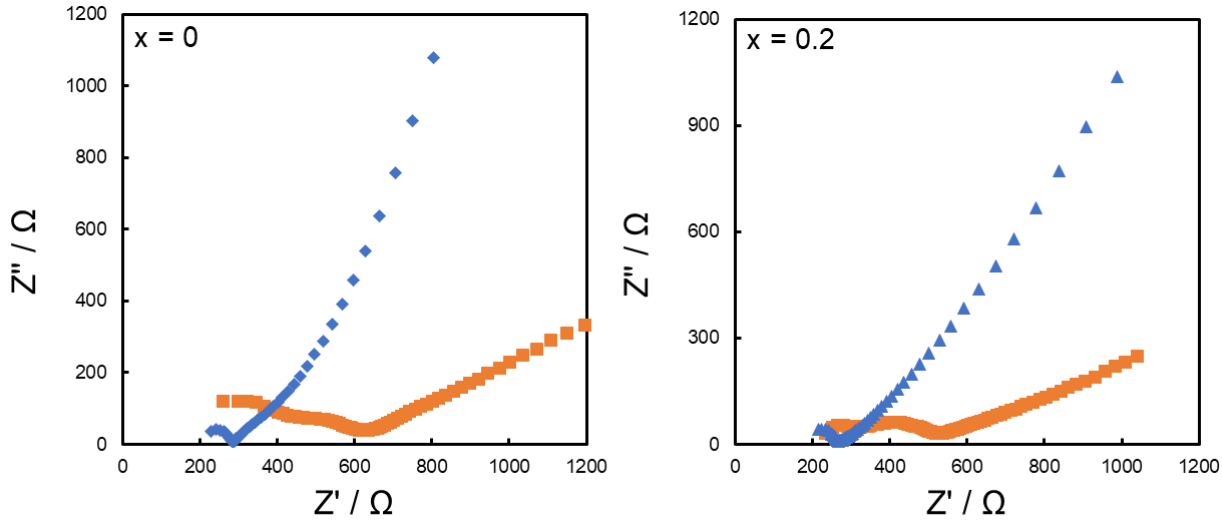

Figure 5.2. The Nyquist plots of Li_xSi / $75Li_2S{\cdot}25P_2S_5$ / Li-In cells, in which (1-x) $Li_7P_2S_8I{\cdot}xTMAI$ (x = 0, 0.2) were used in the Li_xSi electrode composite before and after 10 cycles.

(a)

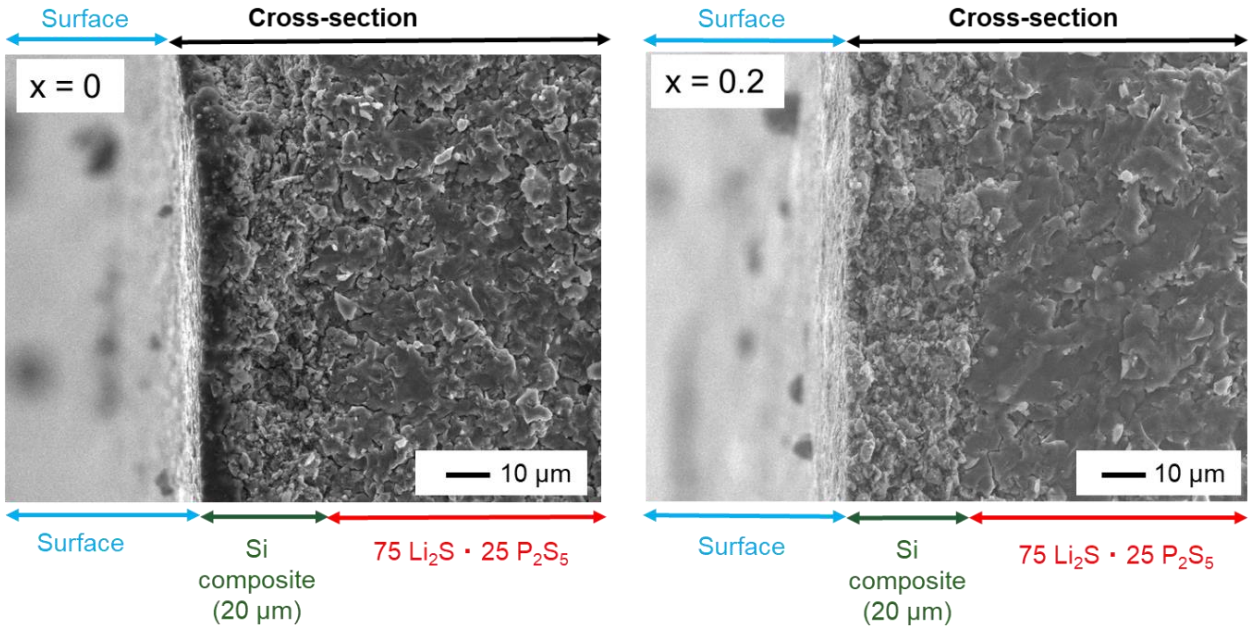
Surface
Cross-section
x = 0
10 μm
Surface
Si composite (20 μm)
75 Li2S · 25 P2S5
Surface
Cross-section
x = 0.2
10 μm
Surface
Si composite (20 μm)
75 Li2S · 25 P2S5

(b)

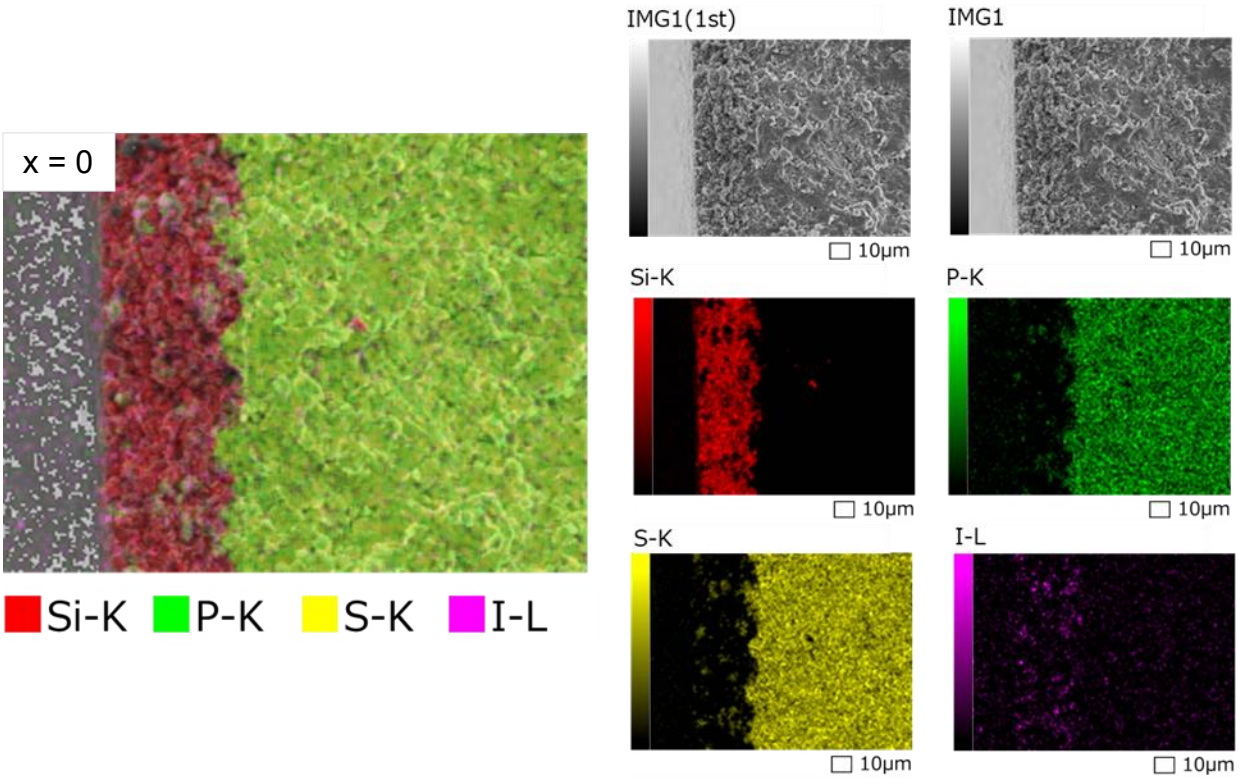
x = 0
Si-K
P-K
S-K
I-L
IMG1(1st)
IMG1
10μm
Si-K
P-K
S-K
I-L

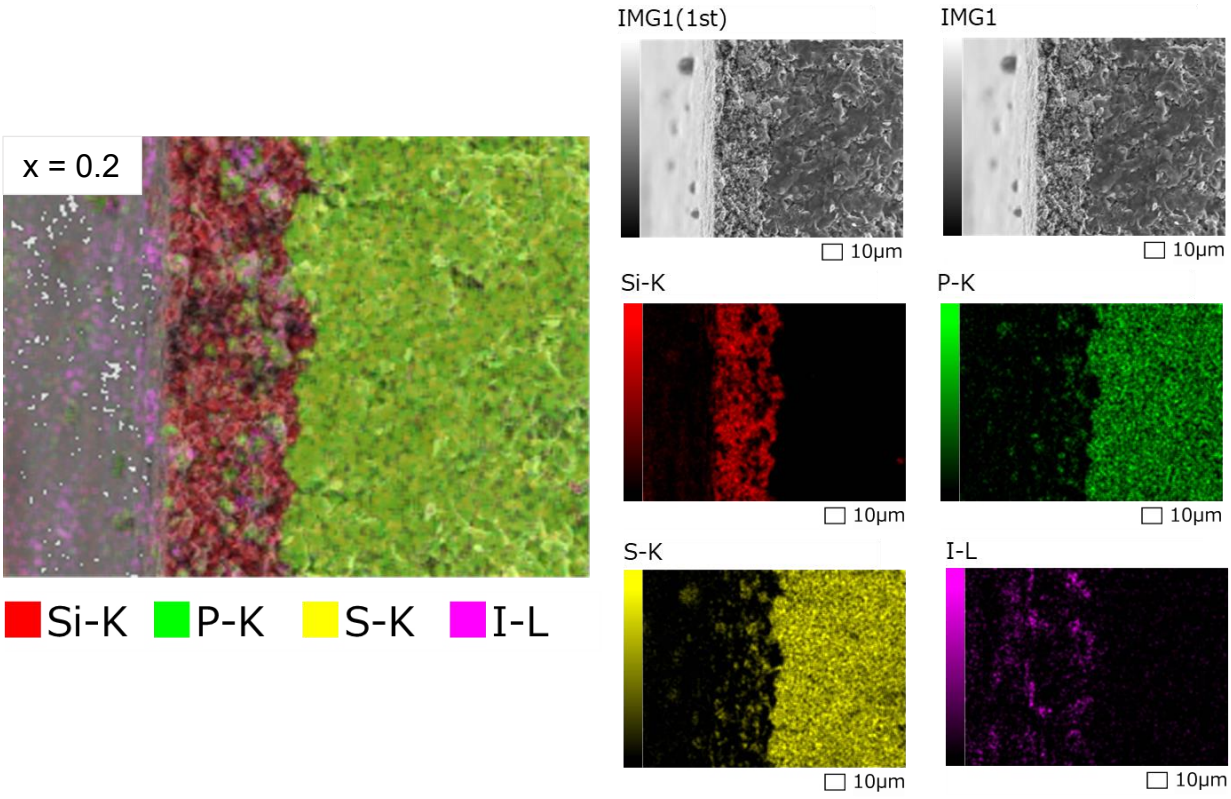

Figure 5.3. The cross-sectional observation of (a) SEM and (b) EDS images before cycling of LixSi · (1-x) $Li_7P_2S_8I$·xTMAI (x = 0, 0.2) / 75Li_2S·25P_2S_5 / Li-In cells.

(a)

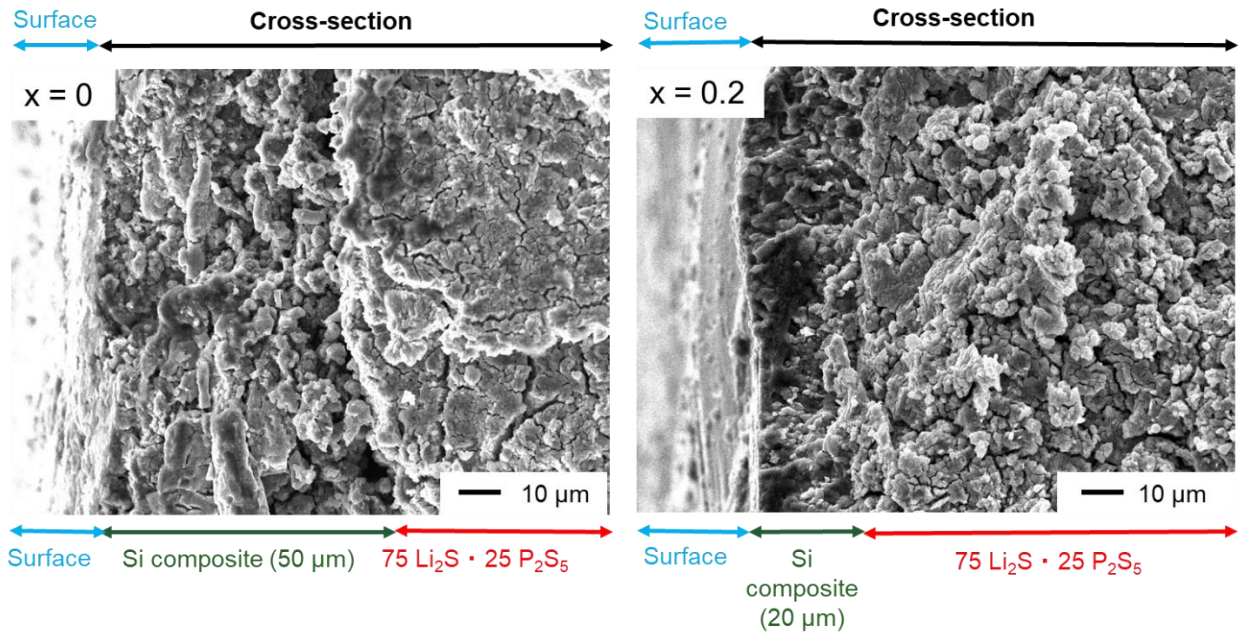
Surface
Cross-section
x = 0
10 μm
Surface
Si composite (50 μm)
75 Li2S・25 P2S5
Surface
Cross-section
x = 0.2
10 μm
Surface
Si composite (20 μm)
75 Li2S・25 P2S5

(b)

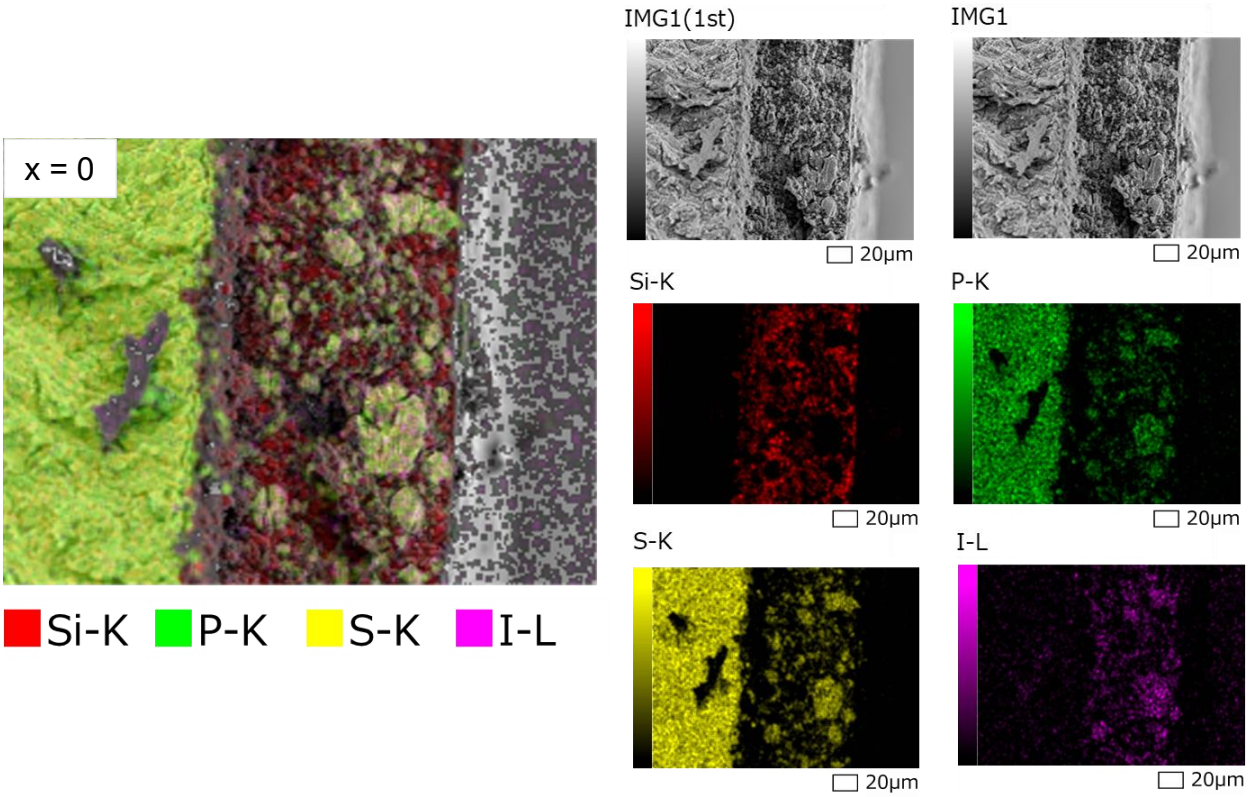
x = 0
Si-K
P-K
S-K
I-L
IMG1(1st)
20μm
IMG1
20μm
Si-K
20μm
P-K
20μm
S-K
20μm
I-L
20μm

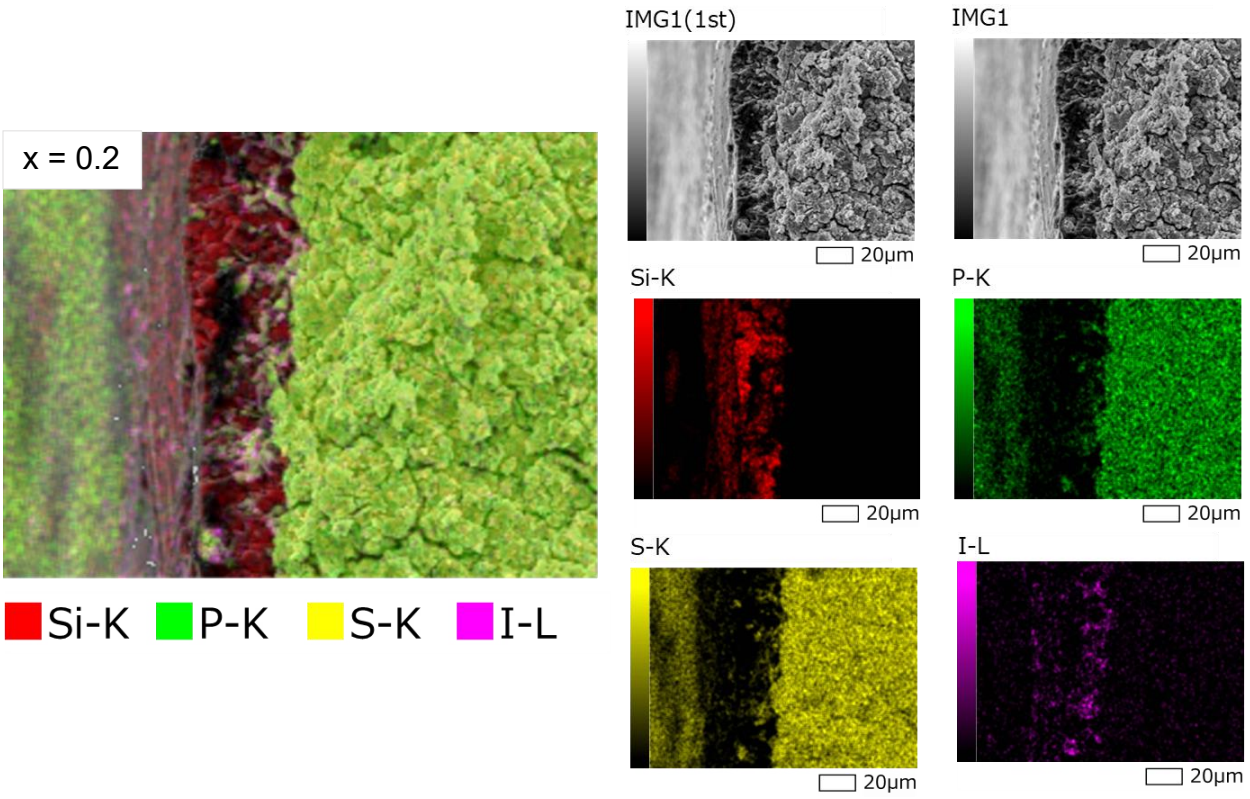

Figure 5.4. The cross-sectional observation of (a) SEM and (b) EDS images after two cycles of LixSi · (1-x) $Li_7P_2S_8I$·xTMAI (x = 0, 0.2) / 75Li_2S·25P_2S_5 / Li-In cells.

5.2.2 Battery Results for $Li_7P_2S_8I$-TEAI, TPAI, TBAI

Due to the excellent battery performance exhibited by the all-solid-state lithium battery containing 0.2 molar fraction of TMAI, I decided to further explore the impact of other large molecular iodide compounds on battery performance. Therefore, I prepared solid-state batteries containing 0.2 molar fractions of TEAI, TPAI, and TBAI and tested their performance, as shown in **Figure 5.5.**

The test results showed that the batteries containing TEAI, TPAI, and TBAI performed worse in cycle performance than those containing TMAI. This phenomenon reveals that battery performance is influenced not only by the softness of the electrolyte material but also by its conductivity. A softer electrolyte material can better adapt to the microstructural changes between electrodes, maintaining good interfacial contact, which is crucial for the long-term cyclic stability of solid-state batteries. However, if the conductivity of the electrolyte is insufficient, even a high degree of softness cannot achieve excellent battery performance.

Moreover, both theoretical analysis and experimental data indicate that the ion conduction mechanism of the electrolyte material significantly affects battery performance. Large molecular iodides such as TEAI, TPAI, and TBAI might hinder ion migration in the electrolyte layer during battery cycling due to their larger molecular structure and relatively lower conductivity, thus affecting the charging and discharging efficiency and cycle life of the battery.

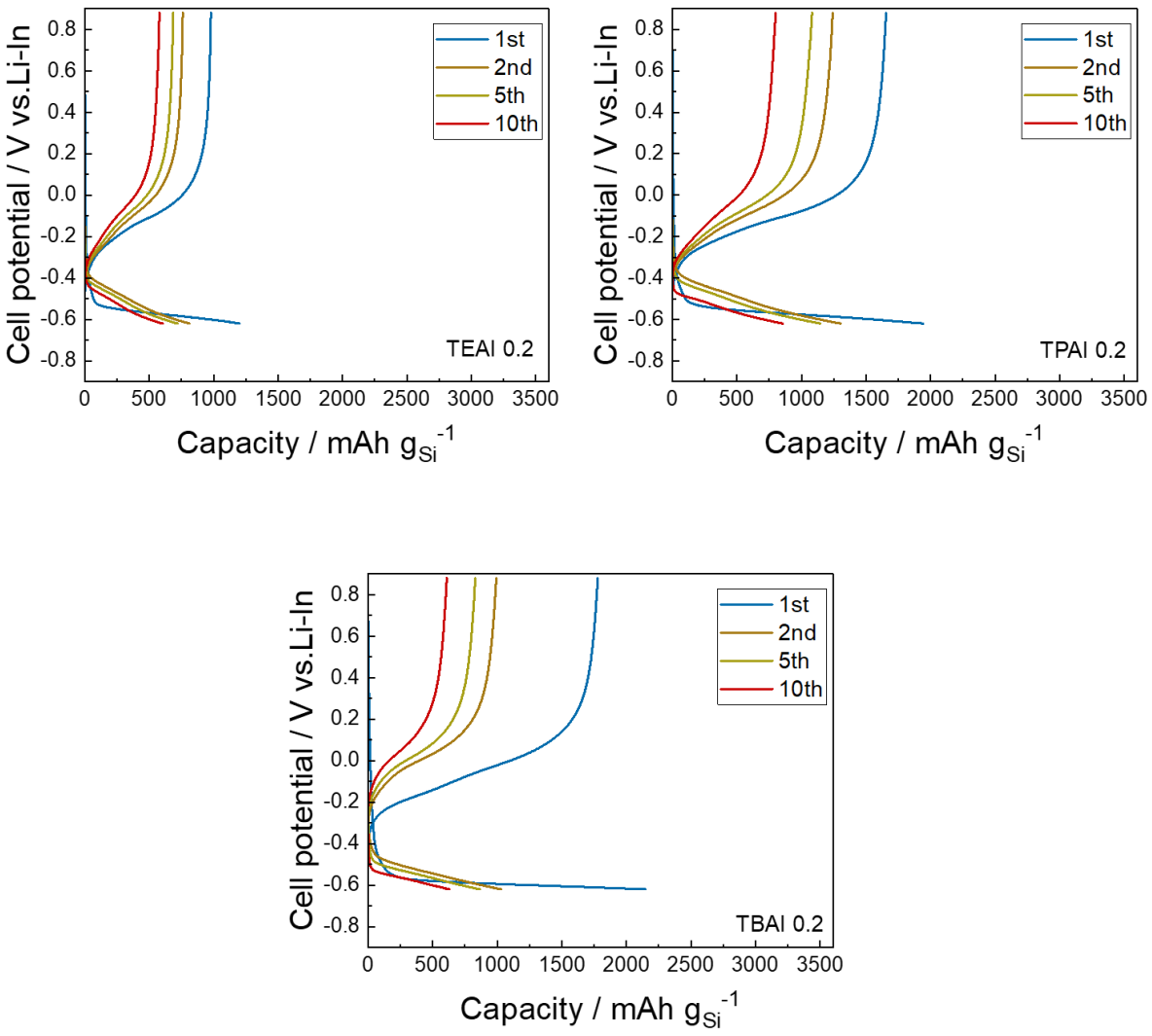

Figure 5.5. The charge-discharge curves of Li_xSi / $75Li_2S{\cdot}25P_2S_5$ / Li-In cells, in which (1-x) $Li_7P_2S_8I{\cdot}x$TEAI, TPAI, TBAI (x = 0.2) were used in the Li_xSi electrode composite.

5.3 Chapter Conclusion

In this chapter, a systematic evaluation was conducted on the performance of various newly developed inorganic-organic hybrid sulfide electrolytes in all-solid-state lithium batteries. The results demonstrate that the addition of TMAI significantly enhanced the cyclic stability of the all-solid-state batteries. Specifically, the sample with x=0.2 TMAI maintained a discharge capacity of 2014 mAh g^{-1} after 10 cycles, showing no significant capacity decay. This improvement is attributed to the enhanced deformability of the solid electrolyte, which effectively mitigated the volume change of the silicon electrode. SEM-EDS observations further confirmed that the electrode composites doped with TMAI remained dense after cycling, indicating their effectiveness in alleviating silicon expansion and preventing electrode cracking.

In contrast, all-solid-state batteries containing 0.2 molar fraction of TEAI, TPAI, and TBAI exhibited lower cycling performance than those doped with TMAI. This highlights the importance of electrolyte deformability and ionic conductivity. While increased deformability helps maintain good interface contact between the electrode and electrolyte, insufficient ionic conductivity still limits overall battery performance. The larger molecular structures and relatively lower conductivity of TEAI, TPAI, and TBAI may hinder ion migration, leading to reduced charge-discharge efficiency and shorter cycle life.

These findings emphasize that the design of effective hybrid sulfide electrolytes must balance mechanical properties and ionic conductivity to achieve optimal battery performance. This chapter provides insights into the complex interactions between the electrolyte and the electrode, which are crucial for ensuring long-term cyclic stability of all-solid-state batteries.

In the upcoming chapters, the mechanical properties of the synthesized hybrid electrolytes are further explored, focusing on the impact of different organic cations on the flexibility, elasticity, and mechanical integrity of the electrolyte layer.

Chapter 6 Evaluation of Mechanical Characteristics

6.1 Introduction

In the previous chapter, the impact of various organic cations on the electrochemical performance of mixed sulfide electrolytes was discussed in detail, particularly in terms of improving the cycling stability of silicon electrodes. The study showed that the introduction of tetramethylammonium iodide (TMAI) significantly enhanced the deformability of the electrolyte, effectively mitigating volume expansion and contraction of the silicon electrode, a crucial factor for achieving long battery cycle life. However, for optimal electrolyte performance, not only high ionic conductivity is necessary, but also robust mechanical properties are essential to withstand physical stresses during charging and discharging.

Solid electrolytes must endure complex mechanical stresses during battery operation, including compression, tension, and shear. Therefore, the mechanical properties of the electrolyte are vital for its long-term stable operation. This chapter focuses on systematic mechanical performance tests of previously synthesized mixed sulfide electrolytes to assess how different organic cations affect their mechanical characteristics.

To gain a deeper understanding of the mechanical behavior of these mixed electrolytes, systematic studies and comparisons were conducted on four different organic cations (TMAI 0.2, TEAI 0.2, TPAI 0.2, and TBAI 0.2). The results of the elasticity modulus tests indicated that the introduction of various organic cations significantly affected the mechanical properties of the electrolytes. Further testing of the elasticity modulus focuses on understanding how the electrolyte materials respond under compression or tension, which is crucial for predicting their performance in actual battery operations.

These mechanical performance tests aim to determine which organic cation can maximize the mechanical stability of the electrolyte without significantly reducing its ionic conductivity. This provides critical experimental evidence and theoretical guidance for optimizing the composition of the electrolyte, aiding in the development of high-energy-density and long-life solid-state lithium batteries.

The findings of this chapter serve as a reference for the development of the next generation of high-performance electrolyte materials. These materials are designed to excel not only in ionic conductivity but also in mechanical properties, enabling them to accommodate the volume changes of electrode materials and various stresses during battery operation, thereby ensuring optimal performance and reliability of solid-state batteries.

6.2 Results and Discussion

The effects of different dopants on the mechanical properties of the sulfide solid electrolyte for (1-x) $Li_7P_2S_8I$ · x (TMAI, TEAI, TPAI, and TBAI) (x = 0, 0.2) samples were evaluated using indentation tests. The compositions of the tested samples were $Li_7P_2S_8I$ (LPSI), TMAI 0.2, TEAI 0.2, TPAI 0.2, and TBAI 0.2. **Figure 6.1** shows the *P-h* curves obtained from 50 repeated indentation-unloading tests on the surfaces of all the samples using a spherical indenter, where *P* is the load applied on the surface of the specimen during the indentation test and *h* is the indentation depth based on the initial surface height of the specimen. According to Hertz's theory.[61]

$$p_m = \frac{P}{\pi R h} = \frac{4}{3}\frac{E}{\pi}\sqrt{\frac{h}{R}}$$

Figure 6.2 showing the Pm-(h/R) $^{1/2}$ Curves for (1-x) $Li_7P_2S_8I \cdot x$ (TMAI, TEAI, TPAI, TBAI) (x = 0, 0.2). According to Hertz's theory, the slope is directly proportional to the elastic modulus. The specific calculations of the elastic modulus are presented in **Table 6.1**, where the introduction of dopants results in changes in the elastic modulus, indicating that the type of dopant has a significant impact on the mechanical properties of the electrolyte.

In the undoped LPSI sample, the elastic modulus is 21.3 GPa, which is consistent with the results of previous studies[16]. After doping with tetraalkylammonium iodides, the decrease in the elastic modulus for TMAI 0.2, TEAI 0.2, and TPAI 0.2 were not quite noticeable, remaining largely consistent with that of undoped LPSI. TBAI 0.2 showed the most significant decrease, with the elastic modulus dropping to 18.4 GPa, which was the lowest among all samples. The doping of TBAI 0.2 significantly lowered the elastic modulus, indicating that long-chain dopants increased the free volume within the glass, loosening the structure, and consequently decreasing the ionic packing density. However, the TEAI 0.2 sample exhibited the highest elastic modulus of 25.2 GPa probably because of the long alkyl chains forming physical cross-linking points within the electrolyte matrix, akin to the network nodes. These cross-linking points improve the structural integrity of the material, as well as enhance its response to external forces, thereby increasing the overall stiffness and elastic modulus. Although longer chain structures may increase the free volume and reduce the elastic modulus, in the case of TEAI, the strengthening effect of physical cross-linking significantly surpasses the softening effect caused by the increased free volume; hence, the TEAI-doped samples displayed a higher elastic modulus. Furthermore, all samples maintained an amorphous state, indicating that doping with tetraalkylammonium iodides did not alter the primary structure of the glass samples. However, the introduction of larger tetraalkylammonium cations increases the free volume within the glass structure. This structural

adjustment allows the material to better accommodate mechanical stresses, such as bending or stretching; thus, better adapting to external deformation while maintaining its original properties, making it more suitable for use in battery technology. Furthermore, it is known that the true density of $70(0.50Li_2S \cdot 0.50P_2S_5) \cdot 30LiI$ is 2.43 g/cm³, which is similar to the density of $Li_7P_2S_8I$. [16] The densities of TMAI, TEAI, TPAI, and TBAI are 1.84 g/cm³, 1.56 g/cm³, approximately 1.31 g/cm³, and 1.2 g/cm³, respectively. Based on the doping levels, I estimated the true densities of (1-x) $Li_7P_2S_8I \cdot x$ (TMAI, TEAI, TPAI, and TBAI) (x = 0, 0.2), as shown in **Table 6.2**. The results show that the relative densities of all samples are similar, ranging from approximately 80% to 85%, with porosities of about 20% to 25%. Therefore, the differences in the measured elastic moduli are mainly due to the intrinsic properties of the materials, rather than variations in porosity.

Table 6.1. Characteristic Properties of Materials Tested with Indentation

Samples	**Elastic Modulus (GPa)**
LPSI	21.3
TMAI 0.2	22.9
TEAI 0.2	25.2
TPAI 0.2	21.8
TBAI 0.2	18.4

Table 6.2. Molded density and relative density of various samples

	True density ($g\ cm^{-3}$)	Molded density ($g\ cm^{-3}$)	Relative density (%)
LPSI	2.43	1.98	81
TMAI 0.2	2.31	1.84	80
TEAI 0.2	2.26	1.94	85
TPAI 0.2	2.21	1.88	85
TBAI 0.2	2.19	1.90	86

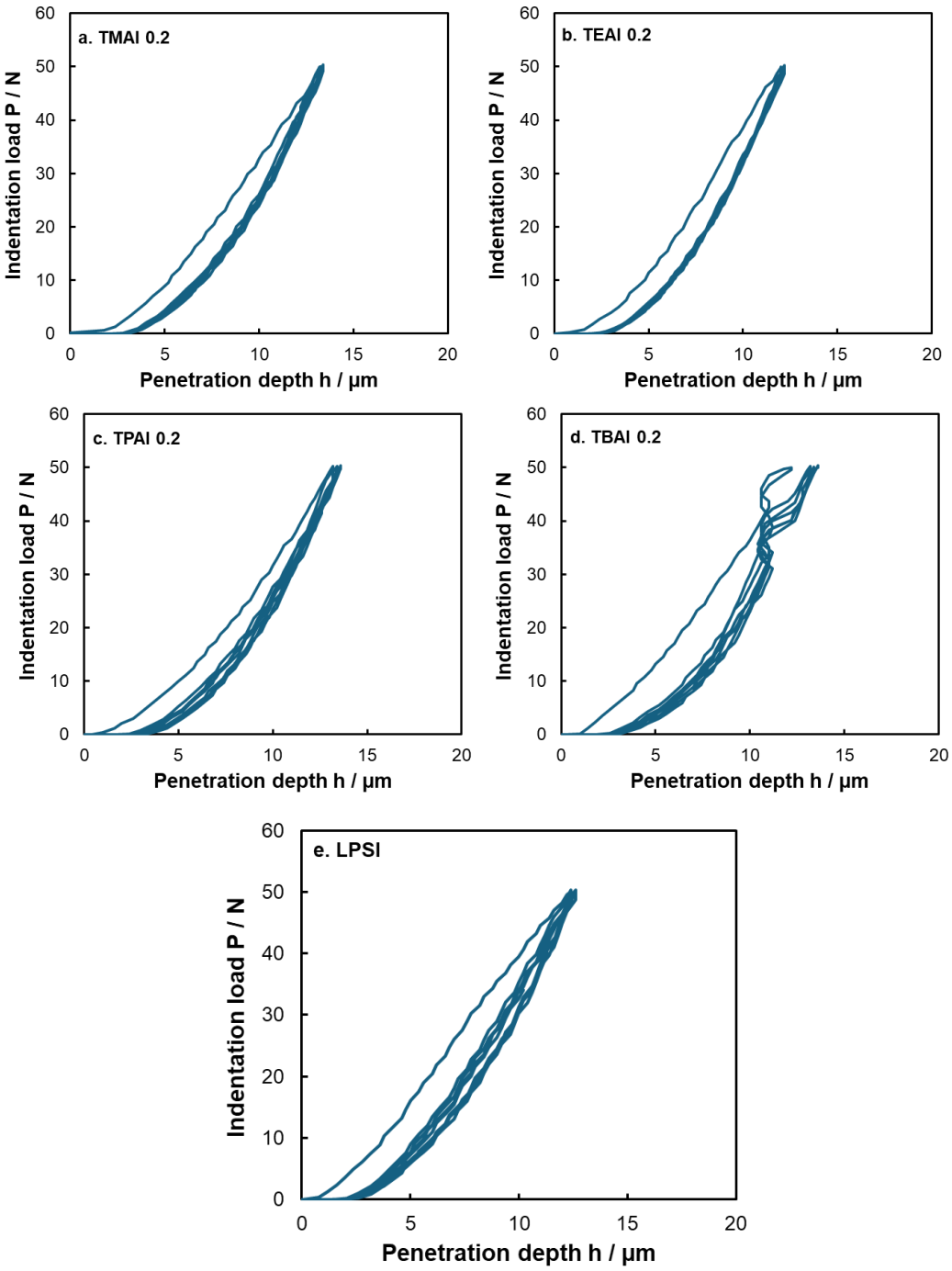

Figure 6.1. *P-h* Curves of (1-x) $Li_7P_2S_8I$ · x (TMAI, TEAI, TPAI, TBAI) (x = 0, 0.2)

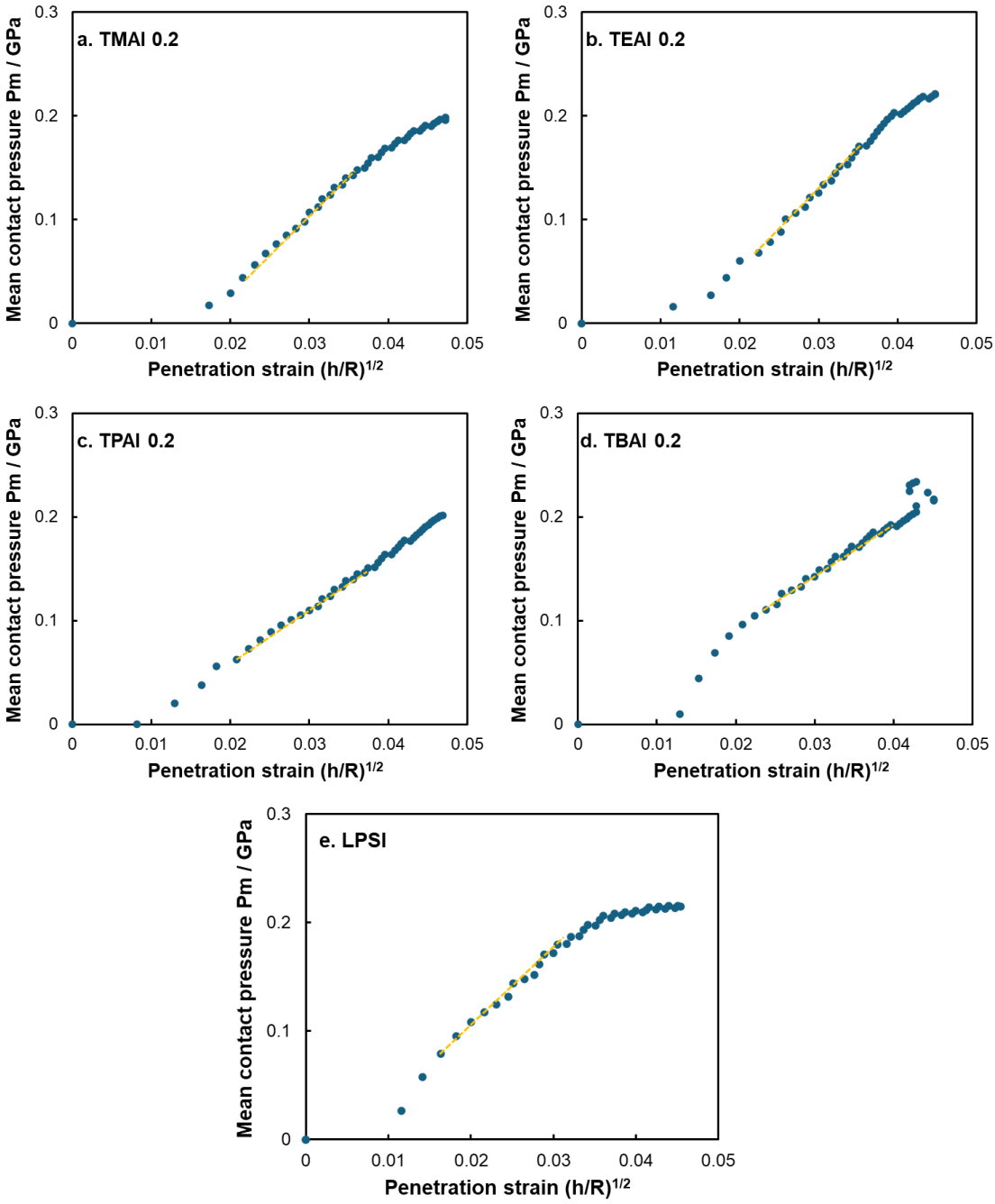

Figure 6.2. Pm-$(h/R)^{1/2}$ Curves of (1-x) $Li_7P_2S_8I \cdot x$ (TMAI, TEAI, TPAI, TBAI) (x = 0, 0.2)

6.3 Chapter Conclusion

The indentation tests conducted on the sulfide solid electrolyte samples, specifically (1-x) $Li_7P_2S_8I$·x (TMAI, TEAI, TPAI, TBAI) with x values of 0 and 0.2, highlighted significant impacts of the dopant type on the mechanical properties of the electrolytes. The tests revealed a distinct variation in the elastic modulus, which is closely linked to the mechanical integrity of the material under stress.

TEAI-doped samples displayed the highest elastic modulus at 25.2 GPa, indicating a robust material capable of withstanding significant mechanical stresses. This enhancement in the elastic modulus is attributed to the formation of physical cross-links within the electrolyte matrix, which reinforce the material's structural rigidity.

On the other hand, TBAI-doped samples showed the lowest elastic modulus, at 18.4 GPa. This reduction is likely due to the increased free volume from the long alkyl chains of TBAI, which introduces more flexibility and less packing density within the matrix. This structural relaxation results in a softer material that may be more susceptible to mechanical deformations under load.

These findings underscore the critical role of dopant selection in tailoring the mechanical properties of solid electrolytes to withstand the stresses encountered during battery operation. While higher elasticity can aid in resisting mechanical deformations, the balance between ionic conductivity and mechanical strength must be carefully managed to optimize battery performance. The research points to the necessity of engineering solid electrolytes that not only exhibit high ionic conductivity but also possess the mechanical robustness required for long-term cyclic stability in battery applications.

Chapter 7 Conclusions

This study systematically evaluated the mechanical and electrochemical performance of inorganic-organic hybrid sulfide solid electrolytes based on (1-x) $Li_7P_2S_8I \cdot x$ (TMAI, TEAI, TPAI, TBAI) (x = 0, 0.05, 0.1, 0.2), exploring their potential applications in all-solid-state lithium batteries. Through detailed investigations of various doped samples, the following main conclusions were drawn:

1. **Structural Consistency of Amorphous State:** Both the undoped and doped samples were confirmed to maintain an amorphous structure, indicating that the introduction of tetraalkylammonium iodides did not disrupt the material's structural characteristics. Preserving the amorphous structure is crucial for ensuring consistent material performance. Additionally, the crystallization temperature of the materials decreased slightly with increasing doping levels, suggesting that the dopant cations are homogeneously distributed within the amorphous matrix.
2. **Influence of Doping on Ionic Conductivity:** The research showed that the type and concentration of the dopant had a noticeable impact on the material's ionic conductivity. Overall, as the doping concentration increased, some samples exhibited a decrease in conductivity, particularly the TBAI series, which showed more complex nonlinear behavior.
3. **Impact of Doping on Mechanical Properties:** The doping of different types of tetraalkylammonium iodides altered the mechanical properties of the sulfide electrolytes. Specifically, samples doped with TEAI exhibited the highest elastic modulus (25.2 GPa), attributed to the formation of physical cross-linking points within the electrolyte matrix

that enhanced structural integrity and resistance to external forces. Conversely, samples doped with TBAI showed the lowest elastic modulus (18.4 GPa), as the longer chain structure increased the material's free volume, leading to a looser structure and reduced mechanical strength.

4. **Improvement in Electrochemical Performance:** The introduction of dopants such as TMAI led to enhancements in the cycle stability and ionic conductivity of all-solid-state batteries. Notably, samples with a TMAI doping concentration of x=0.2 maintained a high discharge capacity after 10 charge-discharge cycles. This improvement is attributed to the doped solid electrolyte materials being better able to accommodate the volume changes of the electrode materials, thus enhancing the overall stability and electrochemical performance of the battery.

In summary, this study investigated the effects of tetraalkylammonium iodide doping on the mechanical and electrochemical properties of sulfide-based solid electrolytes, demonstrating their potential viability in all-solid-state lithium batteries. The findings contribute valuable insights into the development of high-performance solid-state batteries and offer a foundation for future advancements in safer and more efficient energy storage technologies.

Acknowledgments

The successful completion of this research could not have been achieved without the generous support and help from many individuals. First and foremost, I extend my deepest gratitude to my supervisor, Professor Tadanaga, for his dedicated guidance and selfless assistance throughout this research journey. His professional insights and encouragement have been invaluable.

I would like to extend special thanks to my peers. Throughout our PhD journey, we supported and encouraged each other as we faced the challenges of research together, and their companionship provided me with invaluable support and assistance.

Additionally, I am thankful to the junior members of our lab, whose enthusiasm and diligence have infused our laboratory with fresh energy. The collaborative spirit and support offered during the experimental process have been deeply appreciated.

Special thanks are due to my family for their unwavering support and understanding throughout my pursuit of this degree. Your concern and encouragement have been fundamental in driving me forward.

Lastly, I acknowledge everyone who has directly or indirectly contributed to the completion of this research. Your support has made this work possible. As I proceed in my scientific career, I am committed to continuing my efforts, seeking new discoveries, and making further contributions to the field of scientific research.

Academic Papers and Research Achievements Published by the Author

1) **Tong Fang**, Francisco Muñoz, Pamela Vargas, Kiyoharu Tadanaga, and Nataly Carolina Rosero Navarro, Electrochemical Performance Study of AlF_3-Containing Lithium Phosphate Glass Electrolytes. *Journal of Power Sources*, 2025, 625: 235640.
2) **Tong Fang**, Kazuhiro Hikima, Hiroyuki Muto, Atsunori Matsuda, Yuta Fujii, Akira Miura and Kiyoharu Tadanaga, Inorganic-Organic Hybrid Sulfide Solid Electrolytes Based on the Tetraalkylammonium Iodide-LiI-Li_2S-P_2S_5 System. *Journal of The Electrochemical Society,* 2024, 171(10): 100522.
3) **Tong Fang**, Hikaru Tokiwa, Akira Miura and Kiyoharu Tadanaga. Inorganic–organic hybrid solid electrolytes in the tetramethylammonium iodide–LiI–Li_2S–P_2S_5 system for all-solid-state lithium batteries, *Sustainable Energy Fuels*, 2023, **7**, 4297-4302.
4) Takashi Tatebayashi, Tomohiro Ishiyama, Takuya Kinoshita, **Tong Fang**, Yang Ren, Khurelbaatar Zagarzusem, Masaya Fujioka, Gaoyang Zhao, Meng Liu, Takahisa Omata, Junji Nishii. High proton conductivity and thermal stability at intermediate temperatures of phosphate glasses and their melts containing rare-earth oxides achieved by high thermal stability of proton carriers, *Solid State Ionics*, 2023, **403**, 116413.
5) Takahisa Omata, Aman Sharma, Takuya Kinoshita, Lssei Suzuki, Tomohiro Ishiyama, Shinji Kohara, Koji Ohara, Madoka Ono, **Tong Fang**, Yang Ren, Masaya Fujioka, Gaoyang Zhao and Junji Nishii. Investigating the role of GeO_2 in enhancing the thermal stability and proton mobility of proton-conducting phosphate glasses. *Journal of Materials Chemistry A*, 2021, **9(36)**, 20595-20606.
6) Atsushi Miyazaki, Takuya Kinoshita, Takashi Tatebayashi, **Tong Fang**, Yang Ren, Tomohiro Ishiyama, Takuya Omata, Masaya Fujioka, Kaiju Hideo, Gaoyang Zhao, Junji

Nishii. Thermal stability and proton conductivity of densely proton injected phosphate glasses containing rare-earth elements. *Journal of Non-Crystalline Solids*. 2020, **541**, 120064.

7) Yang Ren, **Tong Fang**, Haiyan He, Yajuan Hu, Yonggui Shi, Jiqiang Jia, Gaoyang Zhao. Fine patterned TiO_2: Nb transparent conducting films prepared by a photochemical etching technique, *Chemical Engineering Journal*. 2020, **380**, 122617.
8) Yang Ren, **Tong Fang**, Ying Gong, Xiaoge Zhou, Gaoyang Zhao, Yun Gao, Jiqiang Jia, Zongfan Duan. Enhanced electrochromic performances and patterning of Ni-Sn oxide films prepared by photosensitive sol-gel method, *Journal of Materials Chemistry C*. 2019, **7(23)**, 6964-6971.

References

(1) Zhang, X.; Cheng, S.; Fu, C.; Yin, G.; Wang, L.; Wu, Y.; Huo, H. Advancements and Challenges in Organic-Inorganic Composite Solid Electrolytes for All-Solid-State Lithium Batteries. *NANO-MICRO LETTERS* **2025**, *17*, Review. DOI: 10.1007/s40820-024-01498-y.

(2) Wu, Z.; Li, X. H.; Zheng, C.; Fan, Z.; Zhang, W. K.; Huang, H.; Gan, Y. P.; Xia, Y.; He, X. P.; Tao, X. Y.; et al. Interfaces in Sulfide Solid Electrolyte-Based All-Solid-State Lithium Batteries: Characterization, Mechanism and Strategy. *Electrochemical Energy Reviews* **2023**, *6* (1), 41, Review. DOI: 10.1007/s41918-022-00176-0.

(3) Wu, X. X.; Ji, G. J.; Wang, J. X.; Zhou, G. M.; Liang, Z. Toward Sustainable All Solid-State Li-Metal Batteries: Perspectives on Battery Technology and Recycling Processes. *Advanced Materials* **2023**, 37, Review; Early Access. DOI: 10.1002/adma.202301540.

(4) Wu, J. H.; Liu, S. F.; Han, F. D.; Yao, X. Y.; Wang, C. S. Lithium/Sulfide All-Solid-State Batteries using Sulfide Electrolytes. *Advanced Materials* **2021**, *33* (6), 31, Review. DOI: 10.1002/adma.202000751.

(5) Sung, J.; Heo, J.; Kim, D. H.; Jo, S.; Ha, Y. C.; Kim, D.; Ahn, S.; Park, J. W. Recent advances in all-solid-state batteries for commercialization. *Materials Chemistry Frontiers* **2024**, 27, Review; Early Access. DOI: 10.1039/d3qm01171b.

(6) Peng, Y.; Xiong, X. S.; Fan, W. J.; Gao, W. J.; Cheng, X. B.; He, J. R.; Fu, L. J.; van Ree, T.; Wang, T.; Wu, Y. P. Strategies to regulate the interface between Li metal anodes and all-solid-state electrolytes. *Materials Chemistry Frontiers* **2024**, 30, Review; Early Access. DOI: 10.1039/d3qm01023f.

(7) Pilyugina, Y.; Kuzmina, E.; Kolosnitsyn, V. Review-Recent Advancements in Sulfide Solid Electrolytes for All-Solid-State Lithium-Sulfur Batteries. *ECS JOURNAL OF SOLID STATE SCIENCE AND TECHNOLOGY* **2024**, *13*, Review. DOI: 10.1149/2162-8777/ad575f.

(8) Machín, A.; Morant, C.; Márquez, F. Advancements and Challenges in Solid-State Battery Technology: An In-Depth Review of Solid Electrolytes and Anode Innovations. *Batteries-Basel* **2024**, *10* (1), 36, Review. DOI: 10.3390/batteries10010029.

(9) Jang, J. Challenges and Improvements of All-Solid-State Batteries. *JOURNAL OF THE KOREAN CHEMICAL SOCIETY-DAEHAN HWAHAK HOE JEE* **2023**, *67*, 165-174, Review. DOI: 10.5012/jkcs.2023.67.3.165.

(10) Chan, C.; Wong, H.; Liang, S.; Sun, M.; Wu, T.; Lu, Q.; Lu, L.; Chen, B.; Huang, B. Electrolyte Developments for All-Solid-State Lithium Batteries: Classifications, Recent Advances and Synthesis Methods. *BATTERIES & SUPERCAPS* **2024**, Review; Early Access. DOI: 10.1002/batt.202400432.

(11) Jia, L. A.; Zhu, J. H.; Zhang, X.; Guo, B. J.; Du, Y. B.; Zhuang, X. D. Li-Solid Electrolyte Interfaces/Interphases in All-Solid-State Li Batteries. *Electrochemical Energy Reviews* **2024**, *7* (1), 48, Review. DOI: 10.1007/s41918-024-00212-1.

(12) Sun, H.; Celadon, A.; Cloutier, S.; Al-Haddad, K.; Sun, S.; Zhang, G. Lithium dendrites in all-solid-state batteries: From formation to suppression. *BATTERY ENERGY* **2024**, *3*, Review. DOI: 10.1002/bte2.20230062.

(13) Luo, H.; Guan, Z.; Wu, C.; Zhu, Y.; Wang, C.; Wang, X.; Guo, D.; Chen, X.; Wang, S. High Performance All-Solid-State Lithium Batteries: Interface Regulation Mechanism. *ADVANCED FUNCTIONAL MATERIALS* **2024**, *34*, Review. DOI: 10.1002/adfm.202407007.

(14) Janek, J.; Zeier, W. A solid future for battery development. *NATURE ENERGY* **2016**, *1*, Editorial Material. DOI: 10.1038/NENERGY.2016.141.

(15) Corporation, T. M. *Idemitsu and Toyota Announce Beginning of Cooperation toward Mass Production of All-Solid-State Batteries for BEVs*. 2023. https://global.toyota/en/newsroom/corporate/39865919.html.

(16) PowerCo, Q. a. *PowerCo and QuantumScape Announce Landmark Agreement to Industrialize Solid-State Batteries*. 2024. https://www.quantumscape.com/announcements.

(17) He, L.; Oh, J.; Chua, J.; Zhou, H. Solid-state electrolytes: Advances and perspectives. *FUNCTIONAL MATERIALS LETTERS* **2021**, *14*, Review. DOI: 10.1142/S1793604721300012.

(18) Xu, L.; Li, J.; Deng, W.; Shuai, H.; Li, S.; Xu, Z.; Li, J.; Hou, H.; Peng, H.; Zou, G.; et al. Garnet Solid Electrolyte for Advanced All-Solid-State Li Batteries. *ADVANCED ENERGY MATERIALS* **2021**, *11*, Review. DOI: 10.1002/aenm.202000648.

(19) Li, P.; Ma, Z. H.; Shi, J.; Han, K.; Wan, Q.; Liu, Y. C.; Qu, X. H. Recent Advances and Perspectives of Air Stable Sulfide-Based Solid Electrolytes for All-Solid-State Lithium Batteries. *Chemical Record* **2022**, *22* (10), 202200086, Review. DOI: 10.1002/tcr.202200086.

(20) Zhang, Q.; Liu, K.; Ding, F.; Liu, X. Recent advances in solid polymer electrolytes for lithium batteries. *NANO RESEARCH* **2017**, *10*, 4139-4174, Review. DOI: 10.1007/s12274-017-1763-4.

(21) Wang, P.; Liu, J.; Cui, W.; Li, X.; Li, Z.; Wan, Y.; Zhang, J.; Long, Y. Electrospinning techniques for inorganic-organic composite electrolytes of all-solid-state lithium metal batteries: a brief review. *JOURNAL OF MATERIALS CHEMISTRY A* **2023**, *11*, 16539-16558, Review. DOI: 10.1039/d3ta02761a.

(22) MERCIER, R.; MALUGANI, J.; FAHYS, B.; ROBERT, G. SUPERIONIC CONDUCTION IN LI2S-P2S5-LII-GLASSES. *SOLID STATE IONICS* **1981**, *5*, 663-666, Article.

(23) Kanno, R.; Maruyama, M. Lithium ionic conductor thio-LISICON -: The Li₂S-GeS₂-P₂S₅ system. *JOURNAL OF THE ELECTROCHEMICAL SOCIETY* **2001**, *148*, A742-A746, Article. DOI: 10.1149/1.1379028.

(24) Mizuno, F.; Hayashi, A.; Tadanaga, K.; Tatsumisago, M. New, highly ion-conductive crystals precipitated from Li₂S-P₂S₅ glasses. *ADVANCED MATERIALS* **2005**, *17*, 918-+, Article.

(25) Yamane, H.; Shibata, M.; Shimane, Y.; Junke, T.; Seino, Y.; Adams, S.; Minami, K.; Hayashi, A.; Tatsumisago, M. Crystal structure of a superionic conductor, Li₇P₃S₁₁. *SOLID STATE IONICS* **2007**, *178*, 1163-1167, Article. DOI: 10.1016/j.ssi.2007.05.020.

(26) Deiseroth, H.; Kong, S.; Eckert, H.; Vannahme, J.; Reiner, C.; Zaiss, T.; Schlosser, M. Li₆PS₅X:: A class of crystalline Li-rich solids with an unusually high Li⁺ mobility. *ANGEWANDTE CHEMIE-INTERNATIONAL EDITION* **2008**, *47*, 755-758, Article. DOI: 10.1002/anie.200703900.

(27) Kamaya, N.; Homma, K.; Yamakawa, Y.; Hirayama, M.; Kanno, R.; Yonemura, M.; Kamiyama, T.; Kato, Y.; Hama, S.; Kawamoto, K.; et al. A lithium superionic conductor. *Nature Materials* **2011**, *10* (9), 682-686, Article. DOI: 10.1038/nmat3066.

(28) Kato, Y.; Hori, S.; Saito, T.; Suzuki, K.; Hirayama, M.; Mitsui, A.; Yonemura, M.; Iba, H.; Kanno, R. High-power all-solid-state batteries using sulfide superionic conductors. *Nature Energy* **2016**, *1*, 16030, Article. DOI: 10.1038/nenergy.2016.30.

(29) Inagaki, M.; Suzuki, K.; Hori, S.; Yoshino, K.; Matsui, N.; Yonemura, M.; Hirayama, M.; Kanno, R. Conduction Mechanism of Li₁₀GeP₂S₁₂-type

Lithium Superionic Conductors in a Li-Sn-Si-P-S System. *CHEMISTRY OF MATERIALS* **2019**, *31*, 3485-3490, Article. DOI: 10.1021/acs.chemmater.9b00743.

(30) Wang, Y.; Yue, J.; Wang, W.; Chen, W.; Zhang, Y.; Yang, Y.; Zhang, J.; Yin, Y.; Zhang, X.; Xin, S.; et al. Constructing a stable interface between the sulfide electrolyte and the Li metal anode via a Li⁺-conductive gel polymer interlayer. *MATERIALS CHEMISTRY FRONTIERS* **2021**, *5* (14), 5328-5335, Article. DOI: 10.1039/d1qm00395j.

(31) Hong, S.; Jang, Y.; Jung, Y.; Cho, W.; Kim, D. Sulfide-Based Flexible Solid Electrolyte Enhancing Cycling Performance of All-Solid-State Lithium Batteries. *ACS APPLIED ENERGY MATERIALS* **2024**, Article; Early Access. DOI: 10.1021/acsaem.4c00547.

(32) Kawamura, J.; Hiyama, S. NEW SUPERIONIC GLASSES BASED ON SILVER-IODIDE WITH ORGANIC MONOMER IONS. *Solid State Ionics* **1992**, *53*, 1227-1231, Article. DOI: 10.1016/0167-2738(92)90317-i.

(33) Tatsumisago, M.; Nagao, M.; Hayashi, A. Recent development of sulfide solid electrolytes and interfacial modification for all-solid-state rechargeable lithium batteries. *Journal of Asian Ceramic Societies* **2013**, *1* (1), 17-25, Review. DOI: 10.1016/j.jascer.2013.03.005.

(34) Oh, P.; Yun, J.; Choi, J. H.; Saqib, K. S.; Embleton, T. J.; Park, S.; Lee, C.; Ali, J.; Ko, K.; Cho, J. Development of High-Energy Anodes for All-Solid-State Lithium Batteries Based on Sulfide Electrolytes. *Angewandte Chemie-International Edition* **2022**, *61* (25), 202201249, Review. DOI: 10.1002/anie.202201249.

(35) Suci, W. G.; Aliwarga, H. K.; Azinuddin, Y. R.; Setyawati, R. B.; Stulasti, K. N. R.; Purwanto, A. Review of various sulfide electrolyte types for solid-state lithium-ion batteries. *Open Engineering* **2022**, *12* (1), 409-423, Review. DOI: 10.1515/eng-2022-0043.

(36) Gurung, A.; Pokharel, J.; Baniya, A.; Pathak, R.; Chen, K.; Lamsal, B. S.; Ghimire, N.; Zhang, W. H.; Zhou, Y.; Qiao, Q. Q. A review on strategies addressing interface incompatibilities in inorganic all-solid-state lithium batteries. *Sustainable Energy & Fuels* **2019**, *3* (12), 3279-3309, Review. DOI: 10.1039/c9se00549h.

(37) Wu, J. H.; Liu, S. F.; Han, F. D.; Yao, X. Y.; Wang, C. S. Lithium/Sulfide All-Solid-State Batteries using Sulfide Electrolytes. *Advanced Materials* **2021**, *33* (6), 2000751, Review. DOI: 10.1002/adma.202000751.

(38) Cao, D. X.; Zhao, Y. Y.; Sun, X.; Natan, A.; Wang, Y.; Xiang, P. Y.; Wang, W.; Zhu, H. L. Processing Strategies to Improve Cell-Level Energy Density of Metal Sulfide Electrolyte-Based All-Solid-State Li Metal Batteries and Beyond. *Acs Energy Letters* **2020**, *5* (11), 3468-3489, Review. DOI: 10.1021/acsenergylett.0c01905.

(39) Liu, D. H.; Bai, Z. Y.; Li, M.; Yu, A. P.; Luo, D.; Liu, W. W.; Yang, L.; Lu, J.; Amine, K.; Chen, Z. W. Developing high safety Li-metal anodes for future high-energy Li-metal batteries: strategies and perspectives. *Chemical Society Reviews* **2020**, *49* (15), 5407-5445, Review. DOI: 10.1039/c9cs00636b.

(40) Minami, K.; Hayashi, A.; Tatsumisago, M. Mechanochemical synthesis of Li2S-P2S5 glass electrolytes with lithium salts. *Solid State Ionics* **2010**, *181* (33-34), 1505-1509, Article. DOI: 10.1016/j.ssi.2010.08.021.

(41) Han, F. D.; Yue, J.; Zhu, X. Y.; Wang, C. S. Suppressing Li Dendrite Formation in Li2S-P2S5 Solid Electrolyte by LiI Incorporation. *Advanced Energy Materials* **2018**, *8* (18), 1703644, Article. DOI: 10.1002/aenm.201703644.

(42) Wu, L. P.; Liu, G. Z.; Wan, H. L.; Weng, W.; Yao, X. Y. Superior lithium-stable Li7P2S8I solid electrolyte for all-solid-state lithium batteries. *Journal of Power Sources* **2021**, *491*, 229565, Article. DOI: 10.1016/j.jpowsour.2021.229565.

(43) Rajagopal, R.; Ryu, K. S. Evaluation of Li6P2S8I solid electrolyte for all solid-state lithium battery applications. *Chemical Engineering Journal* **2020**, *402*, 126179, Article. DOI: 10.1016/j.cej.2020.126179.

(44) Sakuda, A.; Hayashi, A.; Tatsumisago, M. Recent progress on interface formation in all-solid-state batteries. *Current Opinion in Electrochemistry* **2017**, *6* (1), 108-114, Review. DOI: 10.1016/j.coelec.2017.10.008.

(45) Maniwa, R.; Calpa, M.; Rosero-Navarro, N. C.; Miura, A.; Tadanaga, K. Synthesis of sulfide solid electrolytes from Li2S and P2S5 in anisole. *Journal of Materials Chemistry A* **2021**, *9* (1), 400-405, Article. DOI: 10.1039/d0ta08658d.

(46) Jin, Y. M.; He, Q. S.; Liu, G. Z.; Gu, Z.; Wu, M.; Sun, T. Y.; Zhang, Z. H.; Huang, L. F.; Yao, X. Y. Fluorinated Li10GeP2S12 Enables Stable All-Solid-State Lithium Batteries. *Advanced Materials* **2023**, 35, 2211047, Article; Early Access. DOI: 10.1002/adma.202211047.

(47) Son, I. H.; Park, J. H.; Kwon, S.; Park, S.; Rummeli, M. H.; Bachmatiuk, A.; Song, H. J.; Ku, J.; Choi, J. W.; Choi, J. M.; et al. Silicon carbide-free graphene growth on silicon for lithium-ion battery with high volumetric energy density. *Nature Communications* **2015**, *6*, 7393, Article. DOI: 10.1038/ncomms8393.

(48) Suyama, M.; Kato, A.; Sakuda, A.; Hayashi, A.; Tatsumisago, M. Lithium dissolution/deposition behavior with Li3PS4-LiI electrolyte for all-solid-state batteries operating at high temperatures. *Electrochimica Acta* **2018**, *286*, 158-162, Article. DOI: 10.1016/j.electacta.2018.07.227.

(49) Sakuda, A.; Yamauchi, A.; Yubuchi, S.; Kitamura, N.; Idemoto, Y.; Hayashi, A.; Tatsumisago, M. Mechanochemically Prepared Li2S-P2S5-LiBH4 Solid Electrolytes with an Argyrodite Structure. *Acs Omega* **2018**, *3* (5), 5453-5458, Article. DOI: 10.1021/acsomega.8b00377.

(50) Zhao, X. L.; Xiang, P.; Wu, J. H.; Liu, Z. Q.; Shen, L.; Liu, G. Z.; Tian, Z. Q.; Chen, L.; Yao, X. Y. Toluene Tolerated Li(9.88)GeP(1.96)Sb(0.04)S(11.8)8Cl(0.12) Solid Electrolyte toward Ultrathin Membranes for All-Solid-State Lithium Batteries. *Nano Letters* **2023**, *23* (1), 227-234, Letter. DOI: 10.1021/acs.nanolett.2c04140.

(51) Rangasamy, E.; Liu, Z. C.; Gobet, M.; Pilar, K.; Sahu, G.; Zhou, W.; Wu, H.; Greenbaum, S.; Liang, C. D. An Iodide-Based Li₇P₂S₈I Superionic Conductor. *Journal of the American Chemical Society* **2015**, *137* (4), 1384-1387, Article. DOI: 10.1021/ja508723m.

(52) Hikima, K.; Ogawa, K.; Muto, H.; Matsuda, A. Li7P2S8I solid electrolytes synthesized by liquid-phase synthesis with improved heat treatment process. *Journal of the Ceramic Society of Japan* **2022**, *130* (4), 299-302, Article. DOI: 10.2109/jc-ersj2.21176.

(53) Zhang, Z.; Han, W. Q. From Liquid to Solid-State Lithium Metal Batteries: Fundamental Issues and Recent Developments. *Nano-Micro Letters* **2024**, *16* (1), 58, Review. DOI: 10.1007/s40820-023-01234-y.

(54) Xie, W. H.; Deng, Z. Y.; Liu, Z. Y.; Famprikis, T.; Butler, K. T.; Canepa, P. Effects of Grain Boundaries and Surfaces on Electronic and Mechanical Properties of Solid Electrolytes. *Advanced Energy Materials* **2024**, 12, Article; Early Access. DOI: 10.1002/aenm.202304230.

(55) Hayashi, A. Development of Sodium-Ion Conducting Sulfide Electrolytes. *Electrochemistry* **2023**, *91* (10), 6, Article. DOI: 10.5796/electrochemistry.23-00096.

(56) Sahoo, P. P.; Güneren, A.; Hudec, B.; Mikolásek, M.; Nada, A.; Precnerová, M.; Micusík, M.; Lencés, Z.; Nádazdy, P.; Fröhlich, K. Stabilization of the Solid-Electrolyte-Interphase Layer and Improvement of the Performance of Silicon-Graphite Anodes by Nanometer-Thick Atomic-Layer-Deposited ZnO Films. *Acs Applied Nano Materials* **2024**, 13, Review; Early Access. DOI: 10.1021/acsanm.3c05066.

(57) Saddique, J.; Wu, M. J.; Ali, W.; Xu, X. X.; Jiang, Z. G.; Tong, L. Y.; Zheng, H.; Hu, W. K. Opportunities and challenges of nano Si/C composites in lithium ion battery: A mini review. *Journal of Alloys and Compounds* **2024**, *978*, 20, Review; Early Access. DOI: 10.1016/j.jallcom.2024.173507.

(58) Liang, X. X.; Ahmad, N.; Zhang, B. J.; Zeng, C. Y.; Cao, X. T.; Dong, Q. X.; Yang, W. Research progress of robust binders with superior mechanical properties for high-performance silicon-based lithium-ion batteries. *Materials Chemistry Frontiers* **2024**, 33, Review; Early Access. DOI: 10.1039/d3qm00839h.

(59) Huo, H. Y.; Jiang, M.; Bai, Y.; Ahmed, S.; Volz, K.; Hartmann, H.; Henss, A.; Singh, C. V.; Raabe, D.; Janek, J. Chemo-mechanical failure mechanisms of the silicon anode in solid-state batteries. *Nature Materials* **2024**, 11, Article; Early Access. DOI: 10.1038/s41563-023-01792-x.

(60) Fang, T.; Tokiwa, H.; Miura, A.; Tadanaga, K. Inorganic-organic hybrid solid electrolytes in the tetramethylammonium iodide-LiI-Li₂S-P₂S₅ system for all-solid-state lithium batteries. *Sustainable Energy & Fuels* **2023**, *7* (17), 4297-4302, Article. DOI: 10.1039/d3se00453h.

(61) Hikima, K.; Totani, M.; Obokata, S.; Muto, H.; Matsuda, A. Mechanical Properties of Sulfide-Type Solid Electrolytes Analyzed by Indentation Methods. *Acs Applied Energy Materials* **2022**, *5* (2), 2349-2355, Article; Early Access. DOI: 10.1021/acsaem.1c03829.

(62) Kato, A.; Yamamoto, M.; Sakuda, A.; Hayashi, A.; Tatsumisago, M. Mechanical properties of sulfide glasses in all-solid-state batteries. *Acs Applied Energy Materials* **2018**, *1* (3), 1002-1007, Article. DOI: 10.1021/acsaem.7b00140.

(63) Song, Y. B.; Baeck, K. H.; Kwak, H.; Lim, H.; Jung, Y. S. Dimensional Strategies for Bridging the Research Gap between Lab-Scale and Potentially Practical All-Solid-State Batteries: The Role of Sulfide Solid Electrolyte Films. *Advanced Energy Materials* **2023**, *13* (32), 36, Review; Early Access. DOI: 10.1002/aenm.202301142.

(64) Zhou, Y.; Doerrer, C.; Kasemchainan, J.; Bruce, P.; Pasta, M.; Hardwick, L. [Observation of Interfacial Degradation of Li₆PS₅Cl against Lithium Metal and LiCoO₂ via In Situ Electrochemical Raman Microscopy]. *BATTERIES & SUPERCAPS* **2020**, *3*, 647-652. DOI: 10.1002/batt.201900218.

(65) Choi, I.; Kim, E.; Jo, Y.; Hong, J.; Sung, J.; Seo, J.; Kim, B.; Park, J.; Lee, Y.; Ha, Y.; et al. [Solvent-engineered synthesis of sulfide solid electrolytes for high performance all-solid-state batteries]. *JOURNAL OF INDUSTRIAL AND ENGINEERING CHEMISTRY* **2023**, *121*, 107-113. DOI: 10.1016/j.jiec.2023.01.012.

(66) Bresson, S.; Bormann, D.; Khelifa, B. [Raman studies of the C-H stretching modes in various cholesteryl alkanoates]. *VIBRATIONAL SPECTROSCOPY* **1998**, *16*, 163-171.